Cool White Dwarfs*

Brad M.S. Hansen
Department of Physics & Astronomy, University of California, Los Angeles, Los Angeles, California 90025; email: hansen@astro.ucla.edu

James Liebert
Steward Observatory, University of Arizona, Tucson, Arizona 85721; email: liebert@as.arizona.edu

Key Words evolution of stars, interiors of stars, atmospheres of stars, white dwarfs, stellar content of the Galaxy

■ **Abstract** Old, cool white dwarfs convey valuable information about the early history of our Galaxy. They have been used to determine the age of the galactic disk, several open clusters, and a globular cluster. We review the current understanding of the physics of cool white dwarfs, including their mass distribution, chemical evolution, magnetism, and cooling. We also examine the role of white dwarfs as tracers of various stellar populations, both in terms of observational searches and theoretical models.

1. INTRODUCTION

White dwarfs are the endpoint of stellar evolution for the vast majority of stars. As such, the galactic population of white dwarf remnants contains valuable information about the early history of our Galaxy, encoded in the luminosities and temperatures of the oldest members. While of great interest, the study of these old white dwarfs has been hampered by their extreme faintness. It is only in recent years, with the advent of large-scale ground-based surveys and deep *Hubble Space Telescope* (*HST*) exposures, that we have begun to probe these populations at the levels necessary to provide interesting constraints.

This review addresses recent observational and theoretical work directed at the study of the oldest and coolest white dwarfs in the Galaxy and their relation to other astrophysically important questions. To that end, we begin with a discussion of the white dwarfs as drawn from a variety of parent populations (Section 2), including a discussion of the recently controversial subject of galactic halo white dwarfs (Section 2.4). Thereafter, we discuss the physical properties of cool white dwarfs (Section 3), building on the earlier review of Weidemann (1990). Of particular

---

*We dedicate this review to the memory of the late Jesse L. Greenstein, who greatly developed the field of cool white dwarfs on the observational side for several decades.

465

interest is the evolution of the spectral properties as a function of temperature (Section 3.3). Finally, we review the theoretical work of recent years dedicated to understanding the meaning of these diverse observations (Section 4). For an introduction to the basic theory of white dwarf cooling, we refer the reader to the previous Annual Reviews article by D'Antona & Mazzitelli (1990), which is still a good reference for the fundamental physics. In Section 4, we cover the necessary additions to that work. A recent theoretical review, organized along more traditional lines, can be found in Fontaine, Brassard & Bergeron (2001). Another comprehensive review of recent developments in white dwarf research, which also includes discussion of hotter white dwarfs, is that of Koester (2002).

2. POPULATIONS

White dwarfs are identified in two ways. For bound stellar systems, such as open clusters or globular clusters, cluster membership (by virtue of a common proper motion) is sufficient to form a color-magnitude diagram and identify the white dwarfs. Even in the absence of a measurable proper motion, an estimate of the number of white dwarfs can be obtained if the density of foreground/background objects can be estimated. Field white dwarfs have traditionally been identified by (*a*) proper motion, (*b*) blue color, and (*c*) the combination of the two—reduced proper motion. A modest number of the coolest white dwarfs were found as companions with common proper motion to brighter stars by workers such as van Biesbroeck. The most important proper motion surveys were those carried out by Willem Luyten, discussed in Section 2.1. Perhaps the most important current imaging survey for the discovery of ultimately thousands of new white dwarfs is the Sloan Digital Sky Survey (SDSS) (York et al. 2000), which also includes a spectroscopic survey. This is discussed in Section 2.2.

Every galactic kinematic population produces white dwarfs; therefore, we need to be mindful of the fact that our proper motion-selected samples may contain contributions from several different populations. Furthermore, white dwarfs with ages $\sim$10 Gyr have L $\sim 2 \times 10^{-5}$ L$_\odot$ and M$_V \sim$ 17 (more detailed calculations are presented in Section 4). Thus, for the current limiting magnitudes of wide-field proper motion surveys (V $\sim$ 21), the distance limits for detection are <100 pc, and no variations due to scale height are detectable. The distinctions between different populations must be drawn entirely from the velocities. The possibility of the admixture of several components must be born in mind as we review the recent observational results.

2.1. The Luyten Palomar Surveys

Until recently, the primary resource for white dwarf hunters was Luyten's mammoth proper motion surveys of the northern sky. The Luyten Half-Second Catalog (LHS) (Luyten 1975) and the New Luyten Two Tenths Catalog (NLTT) (Luyten

1979–1980) were based primarily on red and blue plates taken with the Palomar Oschin Schmidt, the first epoch being the set taken in the early 1950s, which became the original Palomar Observatory Sky Survey (POSS I). The second epoch were the red-only images obtained by Luyten in the mid-1960s. Covering approximately two thirds of the sky, with proper motions $\mu > 0.5'' \cdot \text{year}^{-1}$, the LHS survey is approximately complete to $R \sim 19$ (Dawson 1986). From this sample, Liebert et al. (1979) and Liebert, Dahn & Monet (1988) drew a sample of cool white dwarfs with $\mu > 0.8'' \cdot \text{year}^{-1}$ and $M_V > 13$, which provided the first evidence for a truncation of the white dwarf luminosity function (LF) due to the finite age of the galactic disk. Even in this very first LF, a handful of stars showed kinematics most likely associated with the halo (Liebert, Dahn & Monet 1984), causing Tamanaha et al. (1990) to study the implications for the white dwarf dark matter hypothesis (see Section 2.4).

The recent interest in the possible existence of halo white dwarfs has prompted several authors to reassess the completeness of Luyten's surveys in order to properly assess the degree to which they constrain the density of high-velocity white dwarfs. Flynn et al. (2001) argued that the completeness of the LHS Survey is only 60% to V $\sim$ 18.5. However, Monet et al. (2000) examined 1378 square degrees at high galactic latitudes, using POSS II plates. They found only one new white dwarf, indicating a completeness of over 90% for the original Luyten sample. They advance a possible explanation for the discrepant Flynn result by noting that the assumption of constant density out to distances corresponding to $\delta\mu = 5$ mas is invalidated by the vertical variation of the galactic density law. Of course, this assessment does not apply to fields lower than galactic latitude 20°, nor to most of the Southern Hemisphere. Fortunately, the new examinations of POSS plates in the galactic plane by Lépine, Shara & Rich (2002) are revealing many new stars of large proper motion in this part of the missing sky.

Improved estimates of the white dwarf space density and LF will be available soon (Dahn et al. 2003). This study extends the white dwarf selection to $\mu > 0.6'' \cdot \text{year}^{-1}$, covering the same fraction of the sky. This increases the sample from 43 to 92 white dwarfs, nearly all with trigonometric parallaxes. Study of the cumulative distribution function of the proper motions in this sample indicates the presence of disk, thick-disk, and halo components, rather than a single population.

Another valuable step toward identifying more white dwarfs from Luyten's material is the matching of the NLTT (with proper motions $\mu > 0.2'' \cdot \text{year}^{-1}$) against the Two Micron Sky Survey (2MASS) point sources, presented by Salim & Gould (2002). At the time of their paper, 2MASS point sources covering only about half of the sky had been released to the public. Hence, this data set can be augmented. These authors construct a reduced proper motion diagram using the 2MASS J band and an estimated photographic "v," constructed from an optimized formula combining the NLTT blue and red photographic magnitudes. This proves to be more accurate in delineating the white dwarfs from main sequence stars than the photographic color used Luyten. While spectroscopic confirmation will test the accuracy of this procedure, the diagram should reduce the overlap with

the high-velocity, metal-poor subdwarfs (or Population II main sequence stars). Salim & Gould have identified 23 white dwarf candidates not previously in the Gliese Catalog of nearby stars, though noting that some of these may prove to be subdwarfs.

2.2. The Sloan Digital Sky Survey

This ongoing survey was originally intended to cover π steradians above approximately galactic latitude $30°$ in five broad optical bands to a depth of $g' \sim 23$. The primary goals of the spectroscopic follow-up observations were to observe the 10^6 brightest galaxies and 10^5 brightest quasars, but a comparable number of stars—many of them white dwarfs—are receiving spectrograph fibers for various reasons. Fan (1999) made detailed predictions of the expected surface brightness of white dwarfs as a function of galactic latitude, assuming published luminosity functions (Liebert, Dahn & Monet 1988); observed spectral energy distributions (Greenstein & Liebert 1990); and made predictions from model atmospheres for pure H and He compositions (Bergeron, Wesemael & Beauchamp 1995). Fan also used this information to predict the loci of the different spectral classes of white dwarfs in various Sloan two-color diagrams.

It is not yet clear whether Fan's surface density predictions will be correct, but the white dwarfs do appear at predicted locations in the two-color diagrams. In Figure 1, the u'-g' versus g'-r' plot shows the H-rich (DA) and He-rich (DO-DB) sequences at $T_{eff} > 8000$ K split primarily by the Balmer jump in the u'-g' color. For cooler white dwarfs, the Balmer jump and hydrogen lines become much weaker, whereas the helium-atmosphere stars are now too cool to show their excited-state He I lines. The sequences merge together and, worse, into the old main-sequence stellar locus, making the identification of weak-featured white dwarfs quite difficult. More accurately, they converge with the metal-poor edge of the stellar distribution, populated by main sequence stars traditionally said to have an "ultraviolet excess" due to reduced heavy-element opacity below 4000 Å. In the other major two-color diagram (Figure 2), the g'-r' versus r'-i' plot, the two sequences are not well distinguished for hot stars, and they again merge into the stellar locus at about the same temperature.

However, most cool, non-DA white dwarfs observed at high signal-to-noise ratios show weak features, either due to carbon molecular (usually C_2) bands or atomic lines (DQ type), or due to lines of heavier elements (Ca, Mg, Na, and Fe, among others, but often only the Ca II doublet just below 4000 Å). As we discuss below, the presence of carbon is due to dredge-up from the carbon-rich core when the convection zone in the overlying helium envelope becomes deep enough. The heavy elements are believed to be accreted from the interstellar medium when the star occasionally encounters a cloud or high gas density region. After some time passes, gravitational diffusion removes these elements from visibility.

When features of either DQ or DZ type become strong, the colors may be distorted substantially. In the first figure, the C_2 band absorption in g' may move
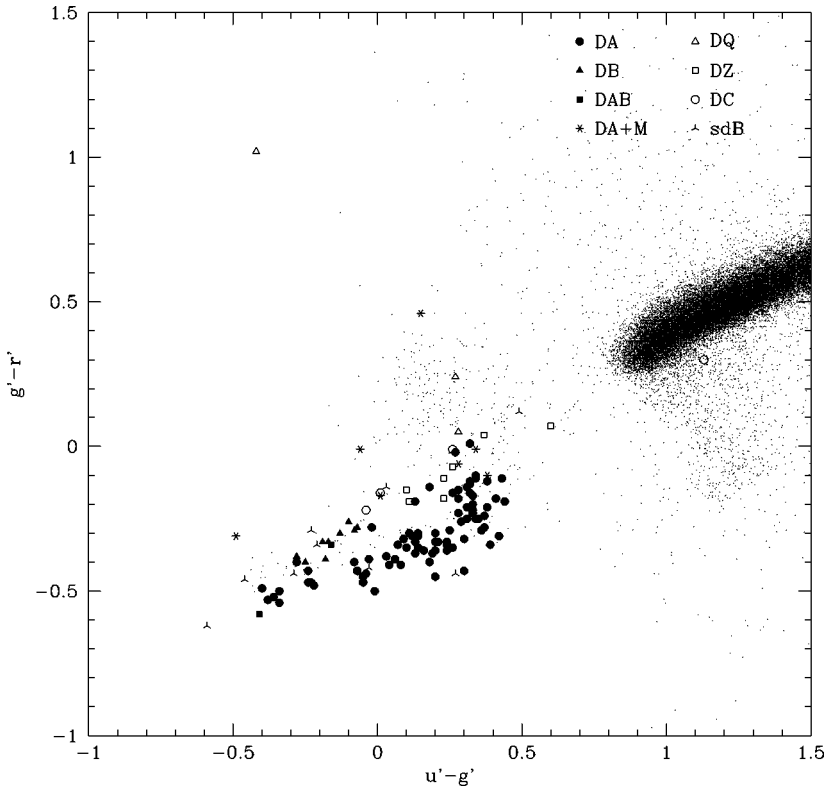
Figure 1 This color-color plot is constructed from the three bluest bandpasses in the Sloan survey. The large grouping at the upper right is the main stellar locus. Hot white dwarfs are bluer than this and lie to the left. Spectroscopically determined white dwarfs are labeled according to their type. (Courtesy of H. Harris.)

the strong DQ stars to the upper left. A strong DZ spectrum with little u' flux moves the color in the opposite direction from the normal locus. Hence, white dwarfs with unusual spectra have been selected because of their unusual colors for spectroscopic observation from the Sloan "serendipity" category. Such white dwarfs appear to be rare, but as they are too cool to show the dominant helium atmospheric constituent, they are necessarily important subsets of the cool white dwarfs. At the coolest temperatures below 5,000 K, however, the frequency of these strong-featured stars seems to decrease, and genuine DC stars with no detectable features become more frequent (along with cool DA stars). These have colors very similar to Population II main sequence subdwarfs, and are the most difficult to find in SDSS or any color survey.

Another group found by unusual color selection are the strongly magnetic white dwarfs, which may show strong and unusual features at almost any wavelength.

Therefore, they can have almost any color! The majority of magnetic white dwarfs, however, have low fields and exhibit only mild Zeeman split lines. These have similar colors to the normal ones of their spectral type.

Finally, some of the coolest of the white dwarfs may move out of the stellar locus due to the presence of extremely strong, collisionally induced absorption (CIA) due to molecular hydrogen, which spreads from the near-infrared to depress the z' and i' bands. Two examples are clearly seen in Figure 2: While showing featureless (DC) spectra, the g'-r' color is extremely red, but the r'-i' color is blue. There was much excitement when these were discovered (Harris et al. 2001—SDSS 1337+ 10) after earlier discoveries of similar objects (Hambly, Smartt & Hodgkin 1997; Hodgkin et al. 2000—WD 0345 + 246; Harris et al. 1999—LHS 3250). At the time of this writing, however, no additional members of this class have been found
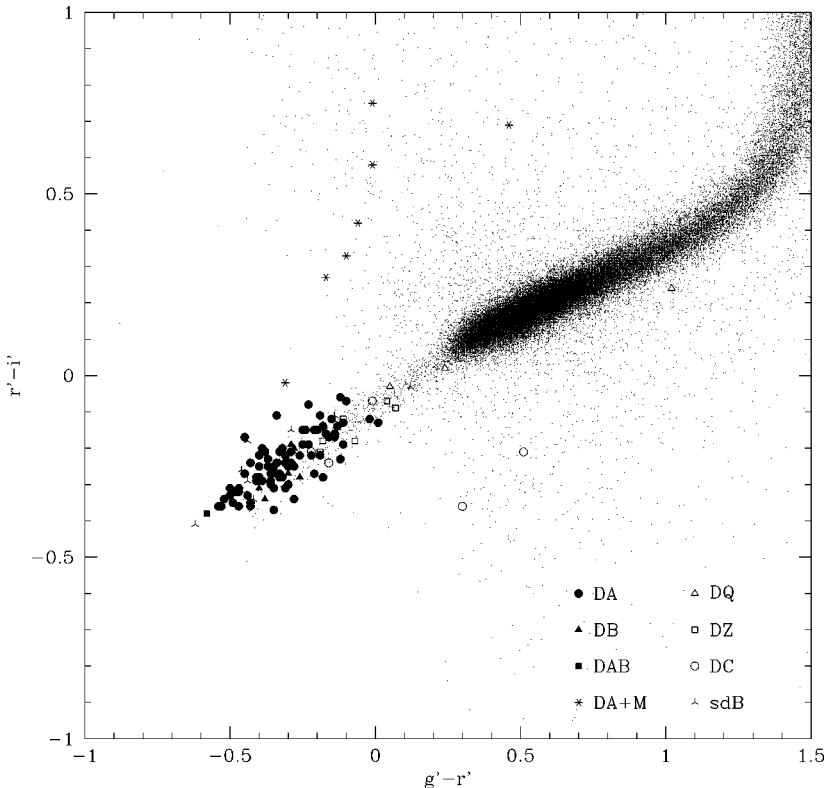

Figure 2 Using the redder bandpasses, the two-color diagram shows a similar topology, with the hot white dwarfs occupying a location blueward of the main stellar grouping. The two "DC" stars lying below the stellar locus (*blue* in r-i) are LHS3250 and SDSS1337 [see Figure 2 of Harris et al. (2001)]. The location of these two stars is because of the infrared absorption by H_2 in the atmosphere. (Courtesy of H. Harris.)

from Sloan data. For the opacity to be this strong, it appears (ironically) that the atmospheric composition must be a mixture of H and He (e.g., Bergeron 2001, Bergeron & Leggett 2002). Unless the temperatures were extremely low (∼2000 K), the hydrogen opacity alone may not be strong enough to produce significant absorption shortward of 1 micron. Further discussion of this phenomenon is taken up in Section 2.4, including the possibility that the coolest halo white dwarfs could show these colors.

However, two of the CIA discoveries appear to show the kinematics of the disk, rather than the halo. Worse, the trigonometric parallax of LHS 3250 (Harris et al. 1999) implies such a high luminosity and radius that its energy distribution must be fit with a mass of 0.23 $M_\odot$ (Bergeron & Leggett 2002). This suggests that the interior is composed of helium, and the object is probably binary (see Section 3.1.2).

In summary, without additional information, such as the measurement of a proper motion, it appears difficult to assemble a complete sample of cool white dwarfs from the SDSS to determine a space density and luminosity function, or even a manageably small subset for follow-up spectroscopic identification. The requirement that the stars be bright enough for detection on the POSS I or the second generation POSS II sky surveys reveals the much greater magnitude limit of the Sloan survey. Moreover, the main sequence subdwarfs have high (halo) tangential velocities and may also have similar proper motions. The color degeneracy problem might be solved by additional imaging near 5100 Å and 6800 Å, where cool subdwarfs show strong molecular hydride bands (Claver 1995).

2.3. Galactic Disk White Dwarfs

The principal objective of the initial efforts was to determine the age of the local galactic disk by measuring the turnover in the white dwarf luminosity function [proposed originally by Schmidt (1959)] and estimating the appropriate age based on white dwarf cooling models. The initial estimate was an age of ∼9 Gyr (Winget et al. 1987), based on the preliminary luminosity function of Liebert et al. (1979). Liebert, Dahn & Monet (1988) present the detailed analysis of the disk white dwarf luminosity function, including the effect that the assumed bolometric corrections have on the nature and location of the turnover. Since the first determination, the pursuit of this goal has been continued with increasing detail. Figure 3 shows the latest developments. The influence of galactic evolution (Iben & Laughlin 1989, Yuan 1989, Wood & Oswalt 1998) has been shown to be secondary to the effect of white dwarf cooling models. A sequence of improved cooling models has been developed by several groups. Wood (1992, 1995) computed models using the best hydrogen-poor and hydrogen-rich models available at the time, finding an age range of 6–13.5 Gyr. Studies discussed in detail below described the possible consequences of the separation of carbon and oxygen during the core crystallization process [building on earlier suggestions of Stevenson (1980)]. The contribution of the separation energy was found to increase the age by ∼1.5 Gyr.

In addition to the studies of cooling theory, Bergeron and collaborators (Bergeron, Wesemael & Fontaine 1992, Bergeron, Saumon & Wesemael 1995) developed detailed models of radiative and convective energy transport in white dwarf atmospheres. These allowed the determination of accurate effective temperatures, gravities, and chemical compositions for individual white dwarfs, culminating in the complete characterization of the individual constituents of the disk luminosity function (Bergeron, Ruiz & Leggett 1997, Leggett, Ruiz & Bergeron 1998, Bergeron, Leggett & Ruiz 2001). The age determined using these parameters and the models of Wood (1995) is 8 ± 1.5 Gyr.

The advances in the atmospheric treatments led to a rather unfortunate mismatch between the detailed atmosphere models used to analyze the observations and the simplified gray atmosphere models used to determine the outer boundary condition in the cooling models. The combined interior + atmosphere models of Hansen (1998, 1999a) were designed to rectify this discrepancy, allowing somewhat lower ages for the disk as a consequence of the sensitivity of the atmospheric boundary condition to the atmospheric composition (total range 6–11 Gyr). Most groups today now incorporate both detailed atmosphere and internal models (Hansen 1999a, Salaris et al. 2000). More detail on this is given in Section 4.

The desire to improve on Luyten-based results has led to several new wide-field surveys. Oswalt et al. (1996) used a survey of wide common-proper motion binaries to define a sample of 50 white dwarfs. The sample is only 10% complete within the limits of $\mu > 0.16'' \cdot \text{year}^{-1}$ and $m_{pg} < 18.5$. Weighting factors are corrected by assuming the distribution with distance in each magnitude bin $\propto \mu^{-3}$ (Smith & Oswalt 1994).[1] Atmospheric composition was determined by interpolation in color tables and, therefore, is more uncertain than the detailed analysis of Leggett et al. (1998). The original comparison with the models of Wood (1995) yielded a disk age of $9.5^{+1.1}_{-0.8}$ Gyr. If the white dwarfs are assumed to all have hydrogen atmospheres, the age jumps to 13 Gyr, whereas, if they are assumed to all have helium atmospheres, the age drops to 9.2 Gyr.

Knox, Hawkins & Hambly (1999) digitally scanned 300 Schmidt plates in ESO/SERC field 287 (originally for a study of quasar variability). Magnitude limits were in the photographic passbands $B_J \sim 22.5$ and $R_F \sim 21.2$. They performed a detailed study of the proper motion limits of the survey, showing reasonable completeness to $\mu_{lim} \sim 50 \, \text{mas} \cdot \text{year}^{-1}$. Follow-up observations were sufficient for spectroscopic confirmation but not enough to unambiguously determine the individual atmospheric compositions (and thus the individual bolometric corrections). Thus, the construction of a bolometric luminosity function requires some assumptions about the statistical distribution of hydrogen and helium atmospheres within the sample. Ages were determined using both the models of Wood (1995) and Garcia-Berro et al. (1996). The overall age range, incorporating both observational and model uncertainties, was 8–14 Gyr.

---

[1]However, this may not hold if the sample contains stars drawn from more than one kinematic population (e.g., Dahn et al. 2003).

The local density of white dwarfs is of interest as a contributor to both halo and disk dark matter. The original determination of Liebert, Dahn & Monet (1988) yielded $\sim 3.3 \times 10^{-3}$ pc^{-3}. Subsequent surveys tend to push this estimate upwards. Knox, Hawkins & Hambly (1999) find a density 4.2×10^{-3} pc^{-3}. Oswalt et al. (1996) find a density of $5.3^{+3.5}_{-0.7} \times 10^{-3}$ pc^{-3} in binaries alone, with an additional contribution from single stars increasing the total to $7.6^{+3.7}_{-0.7} \times 10^{-3}$ pc^{-3}. Festin (1998) used dark nebulae in the Orion, Serpens, & ρ Oph clouds as opaque outer screens to limit the observational volume. The detection of seven white dwarfs in the 464 pc^3 yields a number density of 0.015 ± 0.006 pc^{-3}. Ruiz & Takamiya (1995) performed a proper motion survey in ESO Selected Areas 207, 439, and 440, discovering eight spectroscopically confirmed white dwarfs in a volume ~ 950 pc^3. This yields a density $\sim 8.4 \pm 2.8 \times 10^{-3}$ pc^{-3}. A recent survey with a different emphasis is that of Majewski & Siegel (2001), whose survey of Selected Area 57, near the North Galactic Cap, is too small an area to address questions about halo white dwarfs, but whose unprecedented astrometric precision ($\mu_{\lim} \sim 1$ mas $\cdot$ year^{-1}) allows them to probe the thin-disk white dwarf population to greater distances than other surveys. The seven clearly detected white dwarfs are slightly larger than expected from the interim starcount model of Reid & Majewski (1993) (4.4 white dwarfs expected) but can be made consistent with other studies if a larger disk vertical scale height is assumed. Finally, Holberg, Oswalt & Sion (2002) simply studied the 109 known white dwarfs within 20 pc of the Sun. They find from the cumulative distribution function that this sample is complete to about 13 pc, and measure the solar neighborhood's white dwarf density to be $\sim 5.0 \pm 0.7 \times 10^{-3}$ pc^{-3}. It remains to be seen how many more white dwarfs within 20 pc will emerge from the 23 candidates identified by Salim & Gould (2002).

2.4. Halo and Thick-Disk White Dwarf Candidates

White dwarfs make an attractive candidate for baryonic dark matter by virtue of their low luminosities. The first strong indications of galactic dark matter (Ostriker & Peebles 1973, Rubin, Ford & Thonnard 1978; Faber & Gallagher 1979) led to the suggestion that faint white dwarfs, left over from an early generation of stars, could compose some fraction of the unseen dynamical mass (Larson 1986, Silk 1991). The measurement of the turnover in the disk luminosity function by Liebert, Dahn & Monet (1988) prompted the first direct constraint (Tamanaha et al. 1990), which found that, for halo ages >12 Gyr, the required dark matter density was consistent with the white dwarf remnants of an early burst of high mass star formation (progenitors in the range 1.5–6 $M_\odot$).

Observations of microlensing in the direction of the Large Magellanic Cloud (LMC) (Alcock et al. 1993, Aubourg et al. 1993) elevated the white dwarf dark matter hypothesis to some prominence. Analysis of the accumulated microlensing database (Alcock et al. 1997, 2000) implies a halo population of 0.5 $M_\odot$ dark objects MACHOs, comprising 8%–20% of the local dark matter density, if the lenses are located in the galactic halo. This has stimulated several attempts to

directly detect the population responsible. We note, however, that Sahu (1994) has argued that the majority of these events are caused by lenses that are themselves located in the LMC. The detection of a lensing event caused by a binary in the Small Magellanic Cloud (SMC) (Afonso et al. 1998) lends support to this hypothesis. So the microlensing optical depth should be considered an upper limit on the potential population of halo white dwarfs.

The observations of the Hubble Deep Field North (HDFN) (Williams et al. 1995) were used by several groups (Flynn, Gould & Bahcall 1996; Elson, Santiago & Gilmore 1996; Méndez et al. 1997) to search for faint stars that might trace the microlensing population. Although the number counts were dominated by galaxies, the population of unresolved sources revealed two populations. One was red, relatively bright by HDFN standards, and consistent with the expected spheroid main sequence population. The second population of blue and faint objects did not fit any known stellar population at the time, most likely explained as unresolved starbursting galaxies at moderate to high redshift. The lack of faint, red objects was used to rule out a significant population of halo white dwarfs.

However, as noted earlier, very cool white dwarfs can deviate substantially from black body appearance once the atmospheric hydrogen begins to form molecules (Mould & Liebert 1978; Bergeron, Saumon & Wesemael 1995). In particular, the molecular absorption leads to sufficient infra-red flux depression that the color evolution eventually reverses, becoming bluer with decreasing temperature (Hansen 1998, Saumon & Jacobsen 1999). In particular, within the context of these new models, the faint blue population was found to be consistent with old, hydrogen atmosphere white dwarfs (Hansen 1998). A second epoch in the HDFN field revealed two of these objects with significant proper motions and a further three with marginal proper motion detections (Ibata et al. 1999). These numbers were consistent with the entire dark halo consisting of hydrogen atmosphere white dwarfs. However, this result was controversial and the data were not optimal (having originally been intended for a high-redshift supernova search and thus taken in the noisier I814 bandpass). A third epoch, taken in the wider F606W bandpass, found four of the five objects to have no significant proper motion. The only remaining proper motion candidate (object 4-141 in the Williams et al. catalogue) decreased from an originally claimed value of 35 ± 8 mas $\cdot$ year^{-1} to a statistically weak 10 ± 4 mas $\cdot$ year^{-1} (Richer 2001). Thus, there is currently no strong evidence to support the existence of white dwarf candidates in the HDFN data. It would nonetheless be prudent to do further astrometric imaging of the Hubble Deep Field South (HDFS) to measure the point sources discussed by Méndez & Minniti (2000) because the surface density of halo stars should be higher in this direction.

The limited field of view of the HDFN limits the degree to which these data can be used to constrain the proposed microlensing scenario. The present best-fit MACHO model requires <20% of the dark matter in the form of white dwarfs. The HDFN nondetection is consistent with this requirement. Wide-field proper motion surveys are necessary to go further. Indeed, significant constraints can be placed using the Luyten surveys (Graff, Laughlin & Freese 1998; Hansen 1999a;

Flynn et al. 2001). In addition, several new surveys have begun to address this problem.

Ibata et al. (2000) describe a combination of three different data sets to emphasize different aspects of the search for faint, fast-moving objects. The first uses a set of UK Schmidt plates with a variety of baselines, yielding an average proper motion range $\mu_{\mathrm{lim}} = 0.5$–$2'' \cdot \mathrm{year}^{-1}$ and with a particular sensitivity to blue objects, such as might be expected for cool hydrogen-atmosphere white dwarfs. The second uses the online APM catalogue (Maddox et al. 1990) to search for high proper motion ($\mu > 1'' \cdot \mathrm{year}^{-1}$) in 24 fields. The third set includes a third epoch of ESO-R plates with the APM catalogue to enable a deeper search. Follow-up observations of 101 candidates yielded 18 confirmed proper motion stars with $\mu > 1'' \cdot \mathrm{year}^{-1}$. Spectroscopic confirmation of these white dwarf candidates has only just begun, but Ibata et al. already report the discovery of a new cool white dwarf F351-50 as well as the rediscovery of LHS 542, another high-velocity white dwarf. The estimated density based on only these two objects is $\sim 7 \times 10^{-4} \mathrm{pc}^{-3}$. De Jong, Kuijken & Neeser (2000) report three promising white dwarf candidates in a pilot search over four square degrees using plates from the ESO imaging survey. This is more than expected for standard disk and spheroid populations. However, spectroscopic identifications are lacking.

The largest new data set has been reported by Oppenheimer et al. (2001a), who used digitized plates from the SuperCosmos Survey (Hambly et al. 2001a,c; Hambly, Irwin & MacGillivray 2001b) to cover 4165 square degrees near the south galactic cap to a limiting magnitude of R59F $= 19.8$ and a limiting proper motion $\mu = 0.33'' \cdot \mathrm{year}^{-1}$. They find 126 candidates in the white dwarf region of the reduced proper motion diagram, i.e., $H_R > 22.5$, where $H_R = m + 5 \log \mu$. Spectroscopic follow up revealed 53 new white dwarfs in addition to the 63 previously catalogued. Lacking a distance estimate, a photometric distance relation was used based on empirical studies and white dwarf model atmospheres. Incorporating this distance estimate, they select 38 white dwarfs with $V_\perp > 94 \mathrm{km} \cdot \mathrm{s}^{-1}$ as high-velocity white dwarf candidates. Taking into account the survey volume and completeness, Oppenheimer et al. (2001a) estimate a local density of $2 \times 10^{-4} \mathrm{pc}^{-3}$ in this population, an order of magnitude larger than the white dwarf density predicted from the standard spheroid (Gould et al. 1998). If not accounted for in traditional populations, these white dwarfs represent 2% of the local dark matter density. Furthermore, Oppenheimer et al. note that the luminosity function continues to increase to the detection limit, i.e., the quoted density is a lower limit.

The Oppenheimer et al. result has been the subject of a flurry of activity since its publication. Reid, Sahu & Hawley (2001) note that the velocity cut, as applied by Oppenheimer et al. (2001a), excludes 96% of the locally determined M dwarf sample. The 20 M dwarfs that pass the cut do not show evidence for the low metallicities characteristic of the halo, but are more likely to be part of the thick disk. Reid et al. suggest that the same may be true of the Oppenheimer et al. (2001a) white dwarf sample. Based purely on the white dwarfs with retrograde motions, which are unlikely to be disk members, Reid et al. suggest a more secure lower

limit of 3×10^{-5} pc^{-3} for the true halo members. Comparison with detailed galactic models (Reylé, Robin & Crézé 2001; Flynn, Holopainen & Holmberg 2002) also suggests that the thick disk is a significant contributor. Flynn et al. find that the expected number of white dwarfs from the thin disk, thick disk, and spheroid in the Oppenheimer et al. (2001a) sample are 60, 21, and 10, respectively, a total of 91 that agrees well with the 97 observed by Oppenheimer et al. A maximum likelihood analysis of the Oppenheimer et al. (2001a) sample (Koopmans & Blandford 2001) also finds contributions from the thick disk and halo (with an estimated halo density of $1.1^{+2.1}_{-0.7} \times 10^{-4}$ pc^{-3}). Assuming a simple spherical logarithmic potential, Koopmans & Blandford infer a density profile n(r) $\propto$ r^{-3} for the halo contribution. In addition to kinematic analyses, the magnitudes of the Oppenheimer et al. samples yield information about the individual white dwarf ages and thus the underlying star formation history. Using a more severe velocity cut ($V_\perp > 167$ km $\cdot$ s^{-1}), Hansen (2001) finds that the highest velocity white dwarfs in the Oppenheimer et al. (2001a) sample do exhibit a luminosity function consistent with the kind of burst population expected of either a dark halo or stellar spheroid population. However, the luminosity function of the white dwarfs with velocities between this cut and the Oppenheimer et al. (2001a) cut is more consistent with a period of extended star formation, such as might reflect a disk population. Bergeron (2003) reaches a similar conclusion based on a study of the photometric properties of the Opennheimer et al. (2001a) sample.

Nelson et al. (2002) report the discovery of seven white dwarf candidates from second epoch observations of 74.8 square arcminutes in the "Groth Strip" with *HST*. The small area of the survey is compensated for by the greater depth (complete to V $\sim$ 26.5). Models of the standard stellar populations predict approximately one detection in the survey, so that the seven detections represent a significant excess. This large number of candidates has no reasonable solution using main sequence isochrones and simple models, suggesting that the detections are split roughly evenly between a thin disk population and a dark halo population, representing 10% of the local mass.

The first results from the EROS proper motion survey (Goldman et al. 2002) find no candidate white dwarfs in the 250 square degrees for which they have three epochs. Goldman et al. note that their cuts in proper motion ($\mu > 0.7'' \cdot$ year^{-1}) and reduced proper motion ($H_V > 22.5$ & $H_I > 21.5$) restrict the constraint to old white dwarfs, $M_V > 16$, and are thus consistent with the above surveys, which do report candidates. The EROS result restricts the fraction of the local dark matter density (assumed to be 8×10^{-3} $M_\odot \cdot$ pc^{-3}) in old halo white dwarfs to be less than 5%–15%, depending on the age and nature of the assumed luminosity function.

Finally, one may simply compare properties such as space motions, luminosities, and ages of Luyten proper motion samples with that of Oppenheimer et al. (2001a). Dahn et al. (2003) find a lot of similarities. Silvestri, Oswalt & Hawley (2002) perform the same kind of analysis on a sample of white dwarfs in common proper motion binaries. The main sequence companions allow them to determine the missing radial velocity component, and they conclude that the thick disk and

TABLE 1 The volume searched by the various surveys, ranked in order of decreasing volume for the oldest white dwarfs

Name	Area (deg)	M_{lim}	μ_{lim} ($'' \cdot yr^{-1}$)	Vol$_1$ (pc^3)	Vol$_2$ (pc^3)	Vol$_3$ (pc^3)
Opp.	4165	19.8 (R59F)	0.33	4.4×10^4 (m)	1.1×10^5 (μ)	1.4×10^4 (μ)
LDM	2.8×10^4	18.4 (V)	0.8	2.2×10^4 (m)	4.9×10^4 (μ)	6.1×10^3 (μ)
Monet	1378	20 (V)	0.4	8.9×10^3 (m)	2.1×10^4 (μ)	2.4×10^3 (μ)
EROS	250	21.5 (V)	0.7	5.6×10^3 (μ)	684 (μ)	86 (μ)
Nelson	0.021	26.5 (V)	0.014	941 (m)	4.2×10^3 (m)	900 (μ)
HDF	1.4×10^{-3}	28 (V)	0.01	582 (m)	1.32×10^3 (μ)	167 (μ)
de Jong	2.5	23 (I)	0.5	150 (μ)	18 (μ)	2.4 (μ)
MS	0.3	21.5 (V)	0.001	15 (m)	60 (m)	244 (m)

not the halo is the likely origin of most of their high-velocity stars, and also those of Oppenheimer et al. (2001a).

To judge the relative merits of the different surveys described above, Table 1 presents the effective detectable volumes for three different representative white dwarfs. The first (option 1), is for a representative spheroid or dark halo white dwarf, with $M_V = 17$ and $200 \, km \cdot s^{-1}$ transverse motion. The second option is for a thick-disk white dwarf, with $M_V \sim 16$ and $V_\perp = 100 \, km \cdot s^{-1}$. The third option is for a representative old thin-disk white dwarf, with $M_V \sim 15$ and $V_\perp = 50 \, km \cdot s^{-1}$. In each case, the volume is denoted as either magnitude limited (m) or proper motion limited (μ). The ordering is in terms of decreasing sensitivity to old halo white dwarfs (option 1). An interesting thing to note is that the top three surveys are all most sensitive to the intermediate, or thick disk, class of white dwarf. In fairness, however, we must also note that many authors use additional criteria (such as transverse velocity or reduced proper motion cuts) to further restrict their samples.

Is it possible to make sense of the conflicting claims about both detection [Oppenheimer et al. (2001a)] and nondetection of halo white dwarfs (Goldman et al. 2002)? If we consider that the Goldman nondetection is consistent with a downward poisson fluctuation corresponding to, on average, two white dwarfs in their 8.9×10^3 pc^3, then this corresponds to a density 2.2×10^{-4} pc^{-3}. Such a density implies ∼10 halo dwarfs in the Oppenheimer survey and 5 in the Liebert, Dahn & Monet (1988) sample, and is perfectly consistent with the claimed detected density (although one is an upper limit and the other a lower limit). However, the age distribution of the white dwarfs is somewhat different and the two numbers are not strictly comparable (Hansen 2001, Goldman et al. 2002). Perhaps the most conservative option is to interpret the EROS density as an upper limit on the number of white dwarfs fainter than the Oppenheimer magnitude limit, so that the upper limit on the halo white dwarf density is ∼5×10^{-4} pc^{-3}.

2.4.1. A REPRESENTATIVE MODEL   Given the controversy surrounding the Oppenheimer results, it is of interest to try and set some of the diverse claims on a common footing. To that end, we define below a simple model of the local Galaxy, using commonly used parameters, and compare it to the various surveys discussed above. It is not our intention to derive new constraints, but rather to illustrate which properties are probed by the current surveys. We shall adopt the kinematics given by Binney & Merrifield (1999).

2.4.1.1. The thin disk   The velocity ellipsoid is $(\sigma_R, \sigma_\phi, \sigma_z) = (34, 21, 18)$ km/s, with an asymmetric drift $\langle v_\phi \rangle = -6$ km/s. We assume a constant star formation rate over the past 10 Gyr, with a Salpeter mass function over the white dwarf progenitor part of the initial mass function (IMF).

2.4.1.2. The thick disk $(\sigma_R, \sigma_\phi, \sigma_z) = (61, 58, 39)$ km/s, with $\langle v_\phi \rangle = -36$ km/s. The star formation history is assumed to be a burst 12-Gyr old. The relative normalization of thick and thin disks is a subject of some dispute. We consider a local density normalization of 5% (in main sequence stars—the assumed burst nature of the thick disk then results in a higher relative fraction of white dwarfs).

2.4.1.3. The spheroid   The stellar halo or spheroid is assumed to be only 0.2% of the total density locally. $(\sigma_R, \sigma_\phi, \sigma_z) = (135, 105, 90)$ km/s, with $\langle v_\phi \rangle = -185$ km/s. The star formation history is assumed to be a burst 12-Gyr old.

Figure 4 shows the resulting population in the proper motion, apparent magnitude domain. Several important points can be noted.

1. The thin- and thick-disk samples are limited primarily by the proper motion threshold, whereas the halo sample is magnitude limited in both the Liebert et al. (1988) and Oppenheimer et al. (2001a) surveys (as noted by Koopmans & Blandford 2001).

2. There is an threshold in reduced proper motion that effectively separates thick-disk and halo stars. For these particular parameters, this threshold is $H_V \sim 24$ (a similar threshold was used by Flynn et al. 2001).

3. The relative number of halo, thick-disk, and thin-disk white dwarfs is a function of magnitude, a consequence both of different star formation histories and kinematic selection biases.

The first illustrative diagram of Figure 4 isn't a completely fair way to analyze the high-velocity white dwarf controversy because Oppenheimer et al. (2001a) applied an additional cut, namely that $V_\perp > 94$ km/s. This cut does indeed remove nearly all of the traditional thin disk, leaving a population consisting primarily of thick-disk and spheroid stars, shown in Figure 5.

The best way to compare these kinds of data with theory is the reduced proper motion diagram (Luyten 1922). Figure 6 shows the distribution of the above model in the reduced proper motion diagram, assuming that R59F $\sim$ V. Also shown are
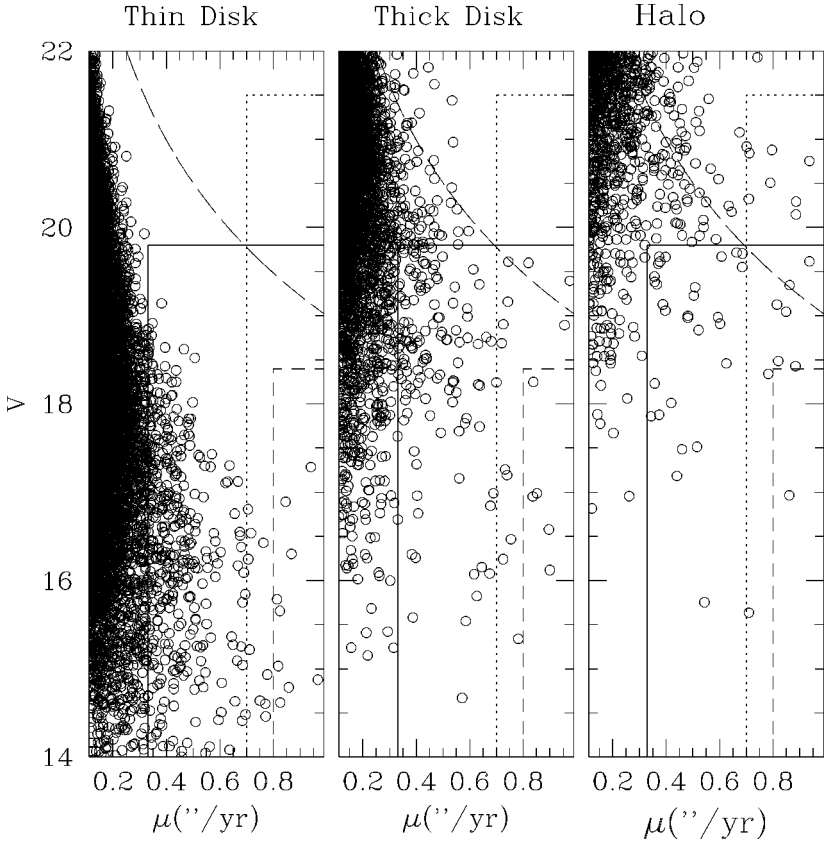
Figure 4   The three panels show, from left to right, the thin-disk, thick-disk, and spheroid (stellar halo) white dwarf populations in μ-V parameter space. The short dashed lines delineate the limit of the Liebert, Dahn & Monet (1988) sample. The dotted lines indicate the EROS2 survey of Goldman et al. The solid line indicates the survey limit of the Oppenheimer et al. (2001a) sample. The long dashed line indicates the reduced proper motion $H_V = 24$. Note that this plot does not indicate the total survey area and, therefore, cannot be used to infer relative numbers of expected detections in the respective surveys. In particular, *HST* surveys cover the entire parameter space shown, although the small field of view limits the number of stars detected.

the data from Oppenheimer et al. (2001a). We see clearly that the Oppenheimer sample consists of a mix of halo and thick-disk stars. The relative fractions will be a function of the model, particularly, the overall normalization and kinematics assumed for the thick disk, especially the amount of asymmetric drift or rotational lag behind the thin disk. Also shown are the Majewski & Siegel (2002) points
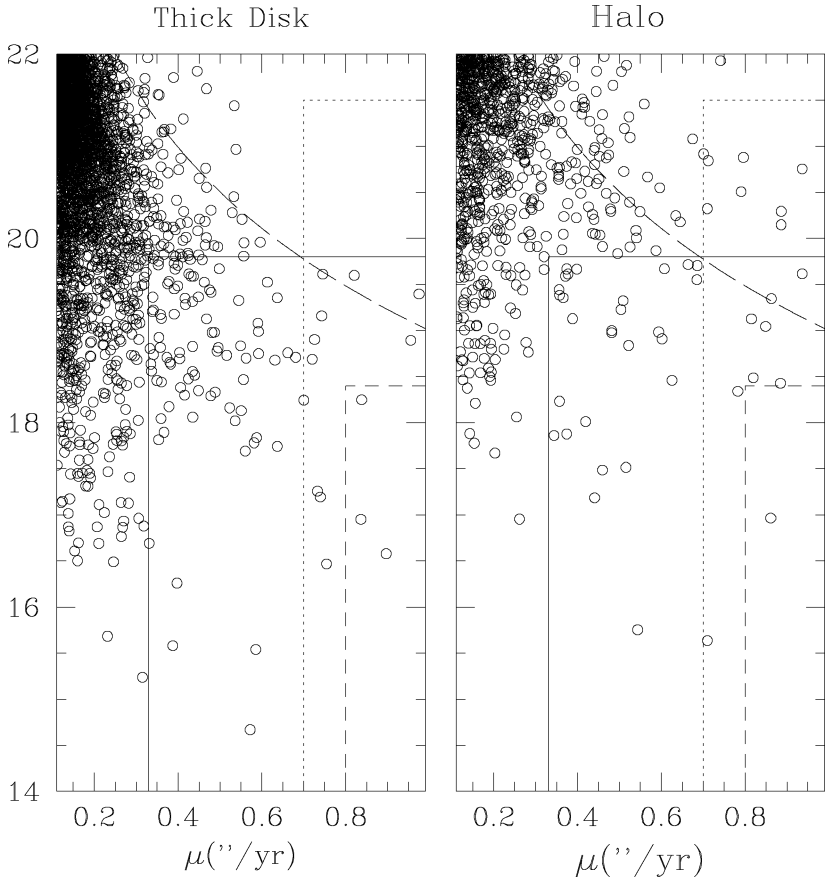
Figure 5   The symbols and lines are as before except that any object with $V_\perp < 94$ km/s has been excluded. We omit the thin-disk diagram, as this population is almost entirely removed by the velocity cut. However, a significant thick-disk contribution remains. For the particular model shown here, only 26% of the thick disk is removed. For a cut of 167 km $\cdot$ s^{-1}, 89% of the thick disk is excluded (as well as 13% of the halo).

(clearly thin disk, as claimed) and the Nelson et al. points, which are also a mix of thick-disk and halo stars.

A final point of interest concerns the "expected" density of spheroid white dwarfs. Once the parameter cuts have been set to confidently exclude contributions from a thick disk, discussions of dark halo white dwarfs must still take into account the contribution from the Galactic stellar halo, or spheroid. Common practice is to cite the expected density from Gould et al. (1998), $\rho \sim 1.3 \times 10^{-5}$ $M_\odot \cdot$ pc^{-3}. However, the authors of that paper noted that there was very little data to constrain the high-mass IMF in the spheroid, and that this number was based on "plausible, if

highly debatable, assumptions." Thus, a density in excess of this value may simply indicate a somewhat flatter spheroid IMF slope than that assumed in Gould et al. ($dN/d\log M \propto M^{-1.7}$). Indeed, if we adopt the minimum high-mass IMF inferred for the population II globular cluster M4 (Richer et al. 2002), then $dN/d\log M \propto M^{-1.1}$ and the expected density is $\rho_{WD} \sim 4.6 \times 10^{-5} \, M_\odot \cdot pc^{-3}$. Also, if one extrapolates the LF of the Dahn et al. (1995) sample of LHS subdwarfs to the white dwarf region, the predicted white dwarf density is $4 \times 10^{-5} \, M_\odot \cdot pc^{-3}$ (Dahn et al. 2003).

The only sure way to separate dark halo from traditional spheroid white dwarfs is to infer a different density profile from a study of the local kinematics (May & Binney 1986, Koopmans & Blandford 2001). However, the motivation behind such a distinction is murky at best. The principal result of the microlensing surveys is to show that the dark matter is not dominated by compact objects. Therefore, the nature of the population giving rise to the observed level of microlensing (even if it lies in the halo) is not constrained by the dynamics to follow the $\rho \propto R^{-2}$ profile assumed for the dark matter.

Indeed, there have been several proposals of intermediate populations comprised solely (or mostly) of white dwarfs that may suffice to explain the microlensing results without contributing significantly to the dark matter. Gyuk & Gates (1999) have investigated a model containing a very thick disk (or "shroud"), which provides the required optical depth in white dwarfs while minimizing the total mass required, in an effort to satisfy various indirect constraints on white dwarf haloes. Inspired by the Oppenheimer et al. results, several groups have proposed dynamical mechanisms to provide a population of high-velocity white dwarfs. Koopmans & Blandford (2001) propose that the widening of a binary orbit, due to mass loss, can drive a hierarchical triple system to dynamical instability, leading to the ejection of the newly formed white dwarf. Davies et al. (2002) propose that most core-collapse supernovae occur in close binaries. The impulse received by the neutron star is sufficient to unbind many of these systems, leaving the original companion with a large systemic velocity resulting from the presupernova orbital velocity. Finally, Hansen (2003) proposes a similar outcome in the case of Type Ia supernovae. In this case, if the supernova mechanism is by the currently favored "single-degenerate" scenario (see Branch et al. 1995 for a review), the presence of a close companion is guaranteed. The mass transfer requirements for the single-degenerate scenario also imply that most of these donor remnants become white dwarfs, resulting in a population with kinematics similar to the thick disk (Hansen 2003). A prediction of all three ejection scenarios is that the ejected population is devoid of binaries.

2.4.2. INDIRECT CONSTRAINTS   The white dwarf contribution to the galactic halo mass can also be constrained by considering the progenitors. An initial mass function truncated from below at 2 $M_\odot$ but extending to 100 $M_\odot$ produces too many heavy elements (Hegyi & Olive 1986). If the upper mass cutoff is reduced to exclude core collapse supernovae, the overall metal production is reduced and can be made consistent with the observational requirements (Ryu et al. 1990, Adams & Laughlin 1996). However, the detailed abundance pattern of halo stars indicates

that carbon and nitrogen are underabundant with respect to oxygen (normalized to the solar value), an enrichment pattern that is not consistent with pollution by white dwarf progenitors, reflecting rather the influence of stars with mass $>15\ M_\odot$ (Gibson & Mould 1997). One potential solution to such an overproduction problem is the ejection of the polluted gas from the Galaxy, such as might occur from a merger-induced starburst-driven wind (Fields, Mathews & Schramm 1997). The implication is that the local group contains $\sim 3 \times 10^{11}\ M_\odot$ of hot gas (kT $\sim$ 0.25 keV), as yet undetected (Fields, Mathews & Schramm 1997). One potential pollution problem that a wind would not fix is the continued production of iron by the merger of halo white dwarf binaries in Type Ia supernovae (Canal, Isern & Ruiz-Lapuente 1997). However, this requires Type Ia supernovae to be the result of white dwarf mergers, which is not necessarily correct (Branch et al. 1995).

Finally, the light emitted by the progenitors of the white dwarfs themselves will affect the high redshift galaxy luminosity function, restricting the white dwarf contribution to total galaxy halo mass to be <20% (Charlot & Silk 1995, Graff et al. 1999). A more comprehensive discussion of the indirect constraints can be found in Koester (2002).

2.4.3. EXOTIC DWARFS Most of the above constraints explicitly assume that any population of "dark halo" white dwarfs have similar properties and progenitor histories as the known population of white dwarfs. If we allow for more extreme possibilities, the constraints can be weakened, at the price of postulating new objects and unknown origins. One possibility is to increase the average mass of the white dwarfs. More massive white dwarfs are brighter at early times but reach crystallization sooner and cool more rapidly thereafter. Similarly, if most of the white dwarfs lose all their surface hydrogen—and do not accrete any more—their cooling can again be accelerated.

An even more extreme example is to consider the structure of very cool, hydrogen-core white dwarfs (Salpeter 1992, Hansen 1999b, Lynden-Bell & Tout 2000). These escape many of the indirect constraints because they have no hydrogen-burning progenitor stage, being formed rather as brown dwarfs that then slowly accreted material cold enough to avoid the onset of nuclear burning. This means they have no bright progenitor stage nor do they leave any kind of chemical pollution. However, the constraints on the formation are quite stringent. If the accretion rate is too high, the accreted material is too hot and the star begins to burn hydrogen, becoming a low-mass star. Such objects are detectable in a deep enough survey, but would be missed by searches that detect the upper branch of the cooling track only, as they cannot populate that part of the color-magnitude diagram (Hansen 1999b).

2.4.4. SUMMARY As we finish this review, it remains an open question what space density of halo white dwarfs have been detected, and what their properties are. There is little doubt that the thick disk accounts for many of the newly discovered halo white dwarf candidates, but the fraction depends sensitively on the

normalization and kinematics assigned to the thick disk component. The need for a dark halo white dwarf contribution based on microlensing events and the Hubble Deep Fields remains dubious. Indeed, the predicted white dwarf density due to the stellar halo/spheroid remains quite uncertain. The implications of recently discovered CIA white dwarfs cooler than 4000 K also remain unclear. WD0346+246 clearly exhibits halo kinematics, but LHS 3250 and SDSS 1337+10 apparently do not. All three of the analyzed stars require high H/He abundance ratios, and the LHS star apparently requires a loss-mass, helium interior, likely resulting from binary evolution. This leaves open the possibility that at least some of these may not simply be interpreted as the closest representatives of the halo population.

2.5. Cluster White Dwarfs

In addition to the studies of field white dwarfs, open and globular clusters offer the opportunity to study the evolution of the white dwarf population in a controlled setting. The estimation of a cluster age using the white dwarf sequence provides an age estimate independent of the main sequence isochrone age, and a comparison of the white dwarf masses with the main sequence turnoff mass can provide constraints on the initial (main sequence) mass–final (white dwarf) mass relation (see Weidemann 1990, Claver et al. 2001 and references therein).

The study of the open cluster cooling sequences has advanced more rapidly than the globular cluster sequences by virtue of their relative proximity and younger ages (hence, brighter white dwarfs). A wide range of clusters have been studied, including (in order of increasing age) NGC 2099 [$t_{wd} = 566^{+154}_{-176}$ Myr, $t_{ms} = 520$ Myr (Kalirai et al. 2001)], NGC 2477 [$t_{wd} > 1$ Gyr, $t_{ms} = 1.2 \pm 0.3$ Gyr (Von Hippel, Gilmore & Jones 1995)], NGC 2420 [$t_{wd} = 2 \pm 0.2$ Gyr, $t_{ms} = 1.5$–3.4 Gyr (Von Hippel & Gilmore 2000)], M67 [$t_{wd} = 4.1 \pm 0.4$ Gyr, $t_{ms} = 4$ Gyr (Richer et al. 1998)], and NGC 188 [$t_{wd} > 4$ Gyr, $t_{ms} = 7$ Gyr (Andreuzzi et al. 2002)]. The comparison of white dwarf and main sequence ages favors those main sequence models that include treatments of convective overshooting (Von Hippel & Gilmore 2000, Kalirai et al. 2001). Comparison of the white dwarf and main sequence populations suggest that white dwarfs contribute roughly 10% of the cluster mass (Von Hippel 1998, Richer et al. 1998).

The detection of white dwarfs in globular clusters has been a long-standing goal. However, early ground-based attempts were hampered by the effects of crowding (Richer & Fahlman 1988). It wasn't until the advent of the *HST* that the first convincing detections were obtained in NGC 6397 (Paresce, de Marchi & Romaniello 1995) and ω Cen (Elson et al. 1995). Detailed sequences have now been detected in NGC 6397 (Cool, Piotto & King 1996), NGC 6752 (Renzini et al. 1996), 47 Tuc (Zoccali et al. 2001), and M4 (Richer et al. 1995, 1997). The white dwarf sequence has been used as a distance indicator (Renzini et al. 1996, Zoccali et al. 2001) by matching the upper part of the cluster cooling sequence to nearby white dwarfs with similar temperatures and well-determined distances, thereby reducing the error on the age determination using the main sequence turnoff. Richer et al.

(1995, 1997) also used the white dwarf cooling sequence directly, placing a lower limit on the age of M4 at 9 Gyr.

Recently, a deep second epoch observation with *HST* was obtained in the outer field of the Richer et al. (1995) M4 study. The goal of this project is a characterization of the entire white dwarf cooling sequence of the globular cluster. Messier 4 is the closest globular cluster and has the advantage over the only other nearby candidate (NGC 6397) in that it is both larger and less dynamically evolved. The two epochs, seperated by almost six years, allow the separation of cluster members from background objects by virtue of the common cluster proper motion [a technique pioneered with *HST* by King et al. (1998)]. Figure 7 shows the proper motion distribution for stars with I > 22 (which contains the
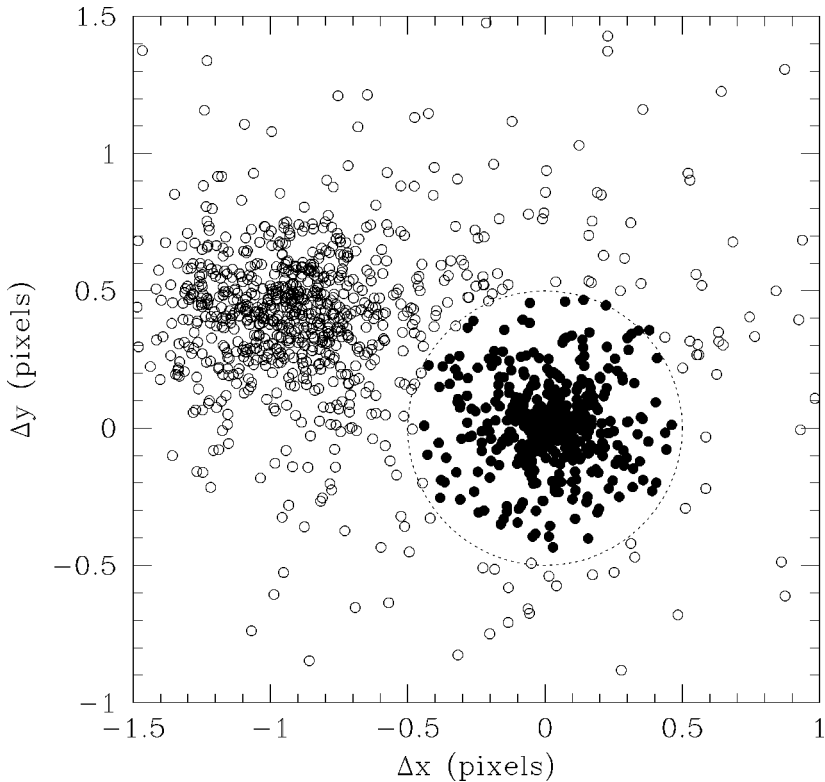
Figure 7 Proper motion displacement diagram from Richer et al. (2002) in the neighborhood of the globular cluster M4. The solid points are designated as cluster members by virtue of having a proper motion displacement with 0.5 WF/PC pixels of the cluster mean displacement (Δx and Δy are defined relative to this mean). The open circles represent field members. Only points with I > 22 are shown.
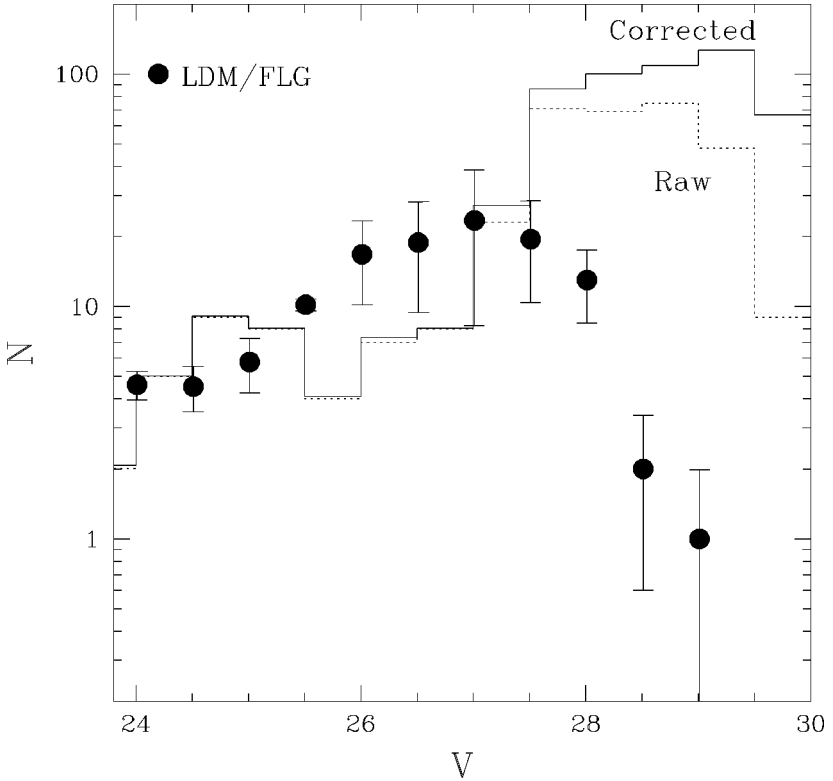
Figure 9   The solid histogram shows the luminosity function for the WDs in M4, corrected for incompleteness. The dashed histogram shows the raw counts. The solid points indicate the disk LF from Leggett, Ruiz & Bergeron (1998), with a V-band distance modulus of $\mu_V = 12.51$ for M4 applied. The vertical normalization is arbitrary—the comparison is designed to demonstrate that the M4 luminosity function extends beyond the turnover in the disk LF, a clear indication that M4 is older than the galactic disk.

entire white dwarf sequence) and Figure 8 shows the resulting cluster white dwarf sequence.

The resulting white dwarf luminosity function (Hansen et al. 2002) is shown in Figure 9, taking into account the incompleteness as a function of magnitude. Also shown is the local disk LF from Leggett et al. (1988), with distance and extinction added to place it at the location of M4. The fact that the cluster luminosity function extends well beyond the turnover in the disk luminosity function is a direct indication that the cluster is older than the local solar neighborhood. The sharp rise in the luminosity function for $I > 26$ is consistent with a single burst of

star formation. Comparison with cooling models yields an age of 12.7 ± 0.7 Gyr (Hansen et al. 2002) and an age difference ~ 3 Gyr between the cluster and the galactic disk. In the current favorite flat, $\Omega_\Lambda = 0.7$, 14 Gyr–old cosmology; this corresponds to cluster formation at $z \sim 6$ and disk formation at $z \sim 1.5$. The number of white dwarfs in the cluster also provide one of the first constraints on the high mass IMF of an old, metal-poor population. The number of observed white dwarfs in the M4 field is roughly equivalent to the observed number of lower main sequence stars and requires a very shallow mass function $dN/dM \propto M^{-0.9 \pm 0.2}$ (Richer et al. 2002).

3. PHYSICAL PROPERTIES

3.1. The Mass Distribution of White Dwarfs

The mass distributions obtained by various techniques indicate strongly that at least three components contribute, probably two of which involve largely close-binary evolution.

3.1.1. THE MEAN MASSES OF HOT AND COOL WHITE DWARFS   Ordinary DA white dwarf atmospheres are believed to be among the most simple among stars because over a wide temperature range they are usually composed only of the simple element, hydrogen. Between approximately 15,000 K, above which the envelopes are not convective, and approximately 40,000 K, above which non-LTE effects exist, trace abundances of heavy elements and helium may become significant; it is generally believed that mass estimates made by fitting log g and T_{eff} to Balmer line profiles are quite accurate. In this manner, Bergeron, Saffer & Liebert (1992) found a narrow peak in the mass distribution just less than 0.6 $M_\odot$, with a dispersion $\sigma(\text{mass}) = 0.137 \, M_\odot$, confirming the result of Koester, Schulz & Weidemann (1979). Later investigations of hot white dwarfs, including those discovered in ROSAT and the Extreme Ultraviolet Explorer (EUVE) surveys, reached similar conclusions about the mean mass (Marsh et al. 1997, Vennes et al. 1997, Finley et al. 1997). These confirmed the similar mean masses from much earlier investigations of Koester, Schulz & Weidemann (1980) and Shipman & Sass (1980), who compared earlier generations of models to observed colors of white dwarfs [see also Weidemann (1990)].

Analyses of cool white dwarfs are plagued by much more complicated physics. In studying cool DA atmospheres, one must confront the uncertain treatment of convection, or at least the free parameters in the mixing length theory (e.g., Bergeron, Wesemael & Fontaine 1992). The derived parameters are found to be sensitive to the parameters of the mixing length theory for $T_{eff} > 9000$ K. Uncertainties also remain in the formulation of the occupation probabilities of hydrogen energy levels in the presence of perturbers (Hummer & Mihalas 1988), or the so-called quenching of the upper levels of a Balmer or Lyman line. For cool non-DA (DC, DQ, DZ) atmospheres, no similar analysis is possible.

However, many more cool white dwarfs have accurate trigonometric parallaxes, and this may be used to estimate the atmospheric and stellar parameters in a different manner, as originally used by Koester, Schulz, & Weidemann (1979). Of course, such determinations are made possible only by the decades of diligent parallax determinations made primarily at the U.S. Naval Observatory, Flagstaff Station. The method was used in the monumental study of cool white dwarfs ($T_{eff} < 10,000$ K) with good parallax determinations by Bergeron, Leggett & Ruiz (2001). Effective temperatures were estimated by fitting the broadband Johnson optical (BVRI) and infrared (JHK) magnitudes once the spectrum has been used to determine whether the dominant atmospheric constituent is hydrogen, helium, mixed, or unclear. The parallax is then used to estimate the luminosity, and from that the radius and mass are estimated.

The mass distribution of cool white dwarfs found in this manner differs somewhat from that for the hotter white dwarfs. The hydrogen-rich subsample has a slightly higher mean of 0.61 $M_\odot$ and a substantially wider dispersion of $\sigma \sim$ 0.20 $M_\odot$; the helium-rich subsample showed a significantly higher mean of 0.72 $M_\odot$ and dispersion of 0.17 $M_\odot$. It is plausible to assume that this method is inherently less accurate than the atmospheric analysis of the hotter stars. Not only do some of the parallaxes have significant errors, but perhaps more importantly, the model physics are not as rigorously known, and the starting T_{eff} determination is arguably far less accurate. Hence, the increased dispersions may be due at least in part to the less accurate values. We revisit the possible reason for a difference in the means between the subsamples in the next section.

Bergeron, Saffer & Liebert (1992) argued that, in addition to the majority of hot DAs having masses very near 0.6 $M_\odot$, separate components of low-mass and high-mass white dwarfs were found.

3.1.2. LOW-MASS WHITE DWARFS Over 10% of the stars measured by the stellar atmospheres method had masses below about 0.5 $M_\odot$, in some cases below 0.4 $M_\odot$. These authors interpreted these as a separate sequence of white dwarfs with helium cores (i.e., because the core mass was below that required for helium ignition), necessarily resulting from binary star evolution. A companion has evidently stripped the envelope from the now-visible white dwarf before it completed its red giant evolution (Kippenhahn, Kohl & Weigert 1967). This hypothesis has been dramatically confirmed by the numerous discoveries of periodic radial velocity variations of the Hα lines of low-mass DA white dwarfs by Marsh, Dhillon & Duck (1995) and Maxted & Marsh (1999) and references therein. There are a few apparent constant-velocity exceptions and a few cases where the companion appears to be an M or L dwarf inferred by infrared excess (Zuckerman & Becklin 1992).

Low-mass white dwarfs are also found in abundance as the companions to millisecond pulsars (Kulkarni 1986; Koester, Chanmugam & Reimers 1992; Bell, Bailes & Bessell 1993; Bailyn 1993; Danziger et al. 1993; Lorimer et al. 1995; Lundgren et al. 1996; van Kerkwijk, Bergeron & Kulkarni 1996; van Kerkwijk et al. 2000) and have been used to constrain the ages and initial spin periods of the

millisecond pulsar companions (Kulkarni 1986, Lorimer et al. 1995, Hansen & Phinney 1998b, Schönberner, Driebe & Blöcker 2000, Althaus et al. 2001a). At the low end of this range ($M < 0.25\ M_\odot$) the white dwarf cooling can be significantly retarded by the residual nuclear burning of hydrogen in a surface shell. The exact mass range affected by this is somewhat sensitive to the treatment of heavy element diffusion and settling in the young white dwarf atmosphere (Webbink 1975, Iben & Tutukov 1986, Alberts et al. 1996, Driebe et al. 1998, Althaus, Serenelli & Benvenuto 2001b).

Another exciting result in low-mass white dwarf studies is the discovery of low-mass white dwarfs in the core of the collapsed globular cluster NGC 6397 (Cool et al. 1998, Edmonds et al. 1999, Taylor et al. 2001). It has been suggested (Castellani, Luridiana & Romaniello 1994; Han, Podsiadlowski & Eggleton 1994) that low-mass white dwarfs may result from single star evolution for low-metallicity populations. However, the fact that these low-mass objects are restricted to the core implies that they are in a binary with a more massive (and dark) companion, either a pulsar or a cool white dwarf (Cool et al. 1998). Consideration of the evolutionary and dynamical history of the system suggests that the companion is most likely a cool white dwarf (Hansen, Kalogera & Rasio 2003).

3.1.3. HIGH-MASS WHITE DWARFS

The high-mass component was delineated clearly in hot DA samples found in the EUVE (Vennes 1999) and ROSAT (Marsh et al. 1997) surveys. These authors argued that more white dwarfs exist with masses larger than $1\ M_\odot$ than allowed for by any reasonable initial mass function and disk star formation model (cf. Yuan 1989, Weidemann 1990). Silvestri et al.'s (2001) radial velocity study of DA white dwarfs led to a conclusion that a second peak near $1\ M_\odot$ is present in the mass function. This conclusion is all the more plausible because of the strong selection bias against such stars in any magnitude-limited survey, where the limiting distance is proportional to the radius of fixed temperature/color. We revisit this issue in the discussion of magnetic white dwarfs.

A plausible argument is that most result from mergers of individual white dwarfs of more ordinary mass, perhaps resulting first in an episode of core helium-burning (Iben & Tutukov 1984a), before returning to the white dwarf sequence as a single object.

Finally, the hot helium DB stars could be observed for similar model atmosphere analysis, with fits to neutral He I lines used as well as the ultraviolet energy distributions (Beauchamp 1996). A sharply peaked mean mass for the DB stars near $0.6\ M_\odot$ was found. The surprising difference is that the DB distribution seems to lack almost entirely the low- and high-mass components. It would seem that binary evolution does not produce DB white dwarfs.

We now return to the apparent difference in mean mass in the cool white dwarf parallax sample of Bergeron, Leggett & Ruiz (2001): A significant representation of high-mass DA and non-DA white dwarfs is present. White dwarfs with apparently very low masses are also present, though these are nearly all of DA type. As Bergeron, Ruiz & Leggett (1997) and Bergeron, Leggett & Ruiz (2001) noted, the

unresolved, binary white dwarfs in this sample may bias the mean mass toward lower than actual values. The method assumes that the observed magnitude and inferred luminosity originate in a single object. If two unresolved stars actually contribute, the inferred radius will be too large and the inferred mass too small. Moreover, if the binaries are predominantly of DA type, the result may be for the mean mass of the DAs to be lower than the actual value. If the non-DA subset is less affected, their inferred mean mass of 0.71 $M_\odot$ may be closer to the true value for all cool white dwarfs.

The Bergeron et al. analysis used cooling tracks with the derived parameters to estimate the age distribution of their sample. These ranged from less than 1 Gyr to at most 9 Gyr. Because at least the older ones more likely originated from a higher mean progenitor mass, it is probably not surprising that the mean mass of such a cool white dwarf sample might be >0.1 $M_\odot$ larger than the hot white dwarf mean.

Massive white dwarfs are also particularly interesting in the context of globular cluster dynamics. The study of dynamically evolved cores of dense globular clusters has found evidence for a rise in the mass-to-light ratio as one approaches the cluster center (Phinney 1993, Dull et al. 1997, D'Amico et al. 2002, Gerssen et al. 2003). There is considerable interest as to whether this rise is due to the presence of a central black hole or a cluster of dark compact remnants, potentially white dwarfs or neutron stars. Neutron stars receive kicks at birth and the retention fraction of neutron stars (Phinney 1993, Drukier 1996, Davies & Hansen 1998) in globular clusters is potentially quite low. White dwarfs of average mass (∼0.5–0.6 $M_\odot$) are less massive than the main sequence turnoff mass and, hence, will not segregate to the core to provide an increase in the central mass-to-light ratio. However, the population of white dwarfs with masses >0.8 $M_\odot$ may segregate and thus has a potentially significant role to play in the dynamical evolution of globular clusters. Neutron stars and stellar mass black holes segregate more by virtue of the greater mass, but white dwarfs have a distinct demographic advantage. This is especially true if the mass function is as shallow as that found in M4 (Richer et al. 2002), namely $x \sim 0.1$, which provides ∼3 times as many white dwarfs per unit main sequence turnoff mass as a Salpeter mass function ($x = 1.35$).

3.2. Tests of Internal Structure

Models of white dwarf stars make several assumptions regarding the composition of the interior and surface layers. While these values are taken from well-constrained stellar models, it is possible to obtain some empirical constraints on the white dwarf interior directly.

The simplest constraint (at least conceptually) is to obtain independent measures of the mass and radius of nearby white dwarfs to test the mass-radius relation. One may perform the classical astrometric tests on nearby white dwarf systems. Current data (Shipman et al. 1998; Provencal et al. 1998, 2002) based on nearby visual binaries, common proper motion binaries, and field white dwarfs supports the mass–radius relation based on carbon/oxygen core models with hydrogen

atmospheres. The demonstration that the previously discrepant system Procyon B (Provencal et al. 1997) is, in fact, a rare DQZ star (whose previous T_{eff} determination was compromised by an unusual atmospheric composition) with a radius consistent with theoretical expectations (Provencal et al. 2002), indicates that this method is capable of stringent tests of the theory (and that it passed).

Another direct measurement of the mass and radius is the gravitational redshift. Bergeron, Liebert & Fulbright (1995) and Reid (1996) compare inferred masses for DA stars from gravitational redshifts with those inferred from spectroscopic, model atmospheres analyses. Generally, the comparisons are favorable for stars hotter than about 12,000–14,000 K. There may be a systematic offset for cooler DA stars due to the problem mentioned in Section 3.3: The spectroscopic method gives a higher mean mass for cooler DA stars than for hotter ones.

Even more powerful constraints can potentially be obtained from asteroseismology. For DA stars with $T_{eff} \sim$ 11,000–12,000 K, when the surface convection zone is small, pulsational variability is observed, and the observation of mode amplitudes and splitting can be used to probe the internal structure of the white dwarf. This method has the prospect of probing the crystalline core of the variable BPM 37093 (Winget et al. 1997, Montgomery & Winget 1999) because the crystalline region is expected to exclude the high shear g–modes that give rise to the observed pulsations. The detection of a period derivative ($P/\dot{P} = 3 \pm 2 \times 10^9$ year) in G117-B15A (Kepler et al. 2000) promises to further probe the interior by direct comparison with internal structure models. The most important contribution from asteroseismology thus far is the constraints on the hydrogen layer masses obtained by detailed analyses. The current data (Bradley 2001 and references therein) show that five out of seven analyzed white dwarfs are consistent with the "standard" model of thick hydrogen and helium layers (having hydrogen/helium mass fractions $q_{He} \sim 10^{-2}$).

The ability of the g-modes to probe the core arguably may place constraints on the core chemical composition. Using an analysis of the $\sim$24,000 K DB pulsator GD358, Metcalfe, Winget & Charbonneau (2001) and Metcalfe, Salaris & Winget (2002) used the mode spectrum to constrain the $^{12}C(\alpha, \gamma)^{16}O$ burning rate. However, a self-consistent treatment of diffusion for evolving white dwarf models led Fontaine & Brassard (2002) to interpret the modes as implying a double-layered envelope—a pure-helium outer envelope and an inner envelope that is a varying mixture of helium, carbon, and oxygen. Moreover, Straniero et al. (2003) warn that the the assumed core chemical distribution is very sensitive to the treatment of convective efficiency in the core helium-burning phase. This uncertainty renders the determination of the reaction rate and central oxygen abundance quite uncertain.

3.3. Spectral Evolution

To further complicate the picture of white dwarf evolution, convincing evidence exists that many of them change their spectral type and atmospheric composition as they age, due to a variety of factors. This could have a dramatic effect on the

cooling rate. We summarize here the complicated and confusing observational evidence, more briefly for the hot white dwarfs.

Post-asymptotic giant branch stars, central stars of planetary nebulae, and hot subdwarfs evolve in two main "channels"—those with H-rich atmospheres and those with He and/or CNO-rich and H-poor atmospheres. These apparently enter either the hot white dwarf stage as DA or PG1159-DO spectral types, respectively. The hot DAs down to about 45,000 K clearly far outnumber the DOs. Moreover, the ratio likely increases with decreasing T_{eff} until 30,000 K, due to the diffusion of residual hydrogen in the envelope to the surface, forming a pure H layer. Indeed, the ratio appears to approach infinity in the 45,000–30,000 K range, the so-called DB gap (Liebert et al. 1986)—there is always enough hydrogen to form an atmosphere. However, below 30,000 K, the helium convection zone has become quite massive, and convective velocities are high enough for overshooting to engulf this outer hydrogen layer if it is thin enough. Over the DB temperature interval (30,000–12,000 K) about one fourth of the DAs convert to DBs, though many may accrete a trace of hydrogen (DBA type). However, as the stars continue to cool below about 11,000 K—the red edge of the pulsating ZZ Ceti instability strip—the relative numbers evolve closer to equality (Sion 1984, Greenstein 1986, Bergeron, Ruiz & Leggett 1997). The likely reason is again convective mixing—this time of the hydrogen envelope into the much more massive helium layer, but again only for those white dwarfs with sufficiently thin hydrogen layers. The higher the layer mass, the cooler the mixing is expected to occur. This convection is invoked as the likely cause of the quenching of the pulsations, whether mixing occurs or not.

For cooler white dwarfs, we have to deal with several complicated, but apparent observational facts, which we summarize below. Again, we draw heavily from the papers of Bergeron, Leggett, and Ruiz—Bergeron, Ruiz & Leggett (1997); Leggett, Ruiz & Bergeron (1998); and Bergeron, Leggett & Ruiz (2001). These provide a systematic study of the spectral classification and individual properties of cool white dwarfs, both in terms of the Liebert, Dahn & Monet (1998) data set (middle reference above) and an expanded set of known, nearby cool stars. An attempt is made below to explain some of these observations in terms of theory.

1. Some cool DAs between about 8,000 to 11,000 K may be partially mixed—enriched in helium up to as much as He:H of unity by number. This is suggested by Bergeron, Leggett & Ruiz (2001) and previously by Bergeron et al. (1990) to account for the higher apparent surface gravities (masses) of these stars relative to hotter DA stars. Dilution of a pure H atmosphere by helium would increase the atmospheric pressure and the apparent gravity. This assumes that the mean mass of the cooler stars should be the same as the hotter DAs.

2. While most cool DA stars below 8,000 K have energy distributions and hydrogen lines fitting pure-H atmospheres, a minority fit atmospheres with He $\gg$ H. These generally show Ca II and may have other lines due to heavy elements (spectral type DZA).

3. While most cool non-DA stars (DC, DQ, DZ) have energy distributions fitting pure-He atmospheres, a minority fit pure-H models, even with the absence of Hα in the spectra.

4. There appears to be a distinct paucity of helium-dominated atmospheres in the T_{eff} range 5,000–6,000 K, termed the non-DA gap by Bergeron, Ruiz & Leggett (1997). However, many DC stars fitting energy distributions of pure-He models are again present below 5,000 K.

5. A puzzling change in the DQ sequence of non-DA stars whose helium envelopes have dredged up carbon appears to occur at similar temperatures. While stars with C_2 bands in their optical spectra occur in the Bergeron samples down to about 6,500 K, below this temperature is where the peculiar DQ stars that may show the C_2H molecule appear (Schmidt, Bergeron & Fegley 1995).

6. About 25% of the cool DAs show detectable Ca II lines in high resolution, high signal-to-noise ratio spectra—type DAZ (Zuckerman et al. 2003). These exist over a wide T_{eff} range and parallel the helium-rich DZ/DZA types, which show broader lines formed in atmospheres at higher pressures.

7. Finally, the only known white dwarfs with T_{eff} below 4,000 K show the infrared (red) flux deficiencies due to H_2 CIA.

The evolution of the atmospheric composition in individual white dwarfs is presumably the result of a complex interaction between accreted material, diffusion of the elements, convective dredge-up and the evolution of the convection zone mass as a function of time and chemical surface composition. This will be discussed in Section 4.3.

Finally, we note that the mean mass of DA and non-DA white dwarfs is similar, taking into account the low-mass white dwarfs that result from binary evolution, which, like their hotter counterparts, seem to all have hydrogen atmospheres.

3.4. Magnetism in Cool White Dwarfs

Magnetic fields have been detected in a minority of white dwarfs, with field strengths spanning the range of tens of kilogauss to nearly 10^9 gauss. The fractional incidence of magnetic white dwarfs has been uncertain because the discovery is complicated by selection effects. Only relatively small samples have been observed with spectropolarimetry, but this is necessary to detect magnetism reliably at strengths below a few megagauss. Fields at and above this value are usually detectable by plain spectroscopy through the Zeeman splitting of stars with lines—if they display lines.

There has been some evidence that fractional incidence, at least of the stronger magnetic fields, is greater among cool white dwarf samples than among hot white dwarfs (Liebert & Sion 1979, Fabrika & Volyavin 1999). This would be disquieting because there is no known way to generate or strengthen magnetic fields in the white dwarf stage of evolution. Instead, the fields should decay with time, albeit

the lowest order dipole component may require gigayears to decline substantially (Fontaine, Thomas & Van Horn 1973). However, the observational samples may be biased, as mentioned before.

At least a partial explanation for this apparent difference in incidence of hot and cool white dwarf samples has been offered by Liebert, Bergeron & Holberg (2003): They showed that the magnetic subset of the Palomar Green sample of hot white dwarfs have a mean mass of 0.93 $M_\odot$, versus the normal mean of around 0.6 $M_\odot$ for white dwarfs (Bergeron, Saffer & Liebert 1992). That many cooler, magnetic white dwarfs have quite high masses was already noted in Liebert (1988). This would mean that for such a cleanly magnitude-limited sample, a substantial bias against the spectroscopic discovery of the magnetic stars exists because their smaller radii allow access to a much smaller search volume than for nonmagnetic white dwarfs. Correction for this effect would help bring the 2% fraction of the PG sample more in line with the around 10% fractions found in samples of cool and nearby white dwarfs studied by Bergeron, Leggett & Ruiz (2001) and Holberg, Oswalt & Sion (2002), respectively (see also Kawka et al. 2003). For at least this last sample of nearby white dwarfs, there is reason to argue that the magnitude limit bias is much reduced. However, this sample nonetheless shows a higher fractional incidence among stars cooler than 10,000 K or older in cooling time greater than 1 Gyr than for hotter or younger white dwarfs. While the statistical significance of this difference is not extremely high, the disquieting issue of possible evolution to higher magnetic field strengths as the white dwarfs age remains unsettled. Observation of a larger, complete sample is required.

4. THEORY

Although we try to make this a comprehensive overview for the nonspecialist, our major emphasis is on developments within the past decade. The reader interested in more details on the early work is directed to the earlier review by D'Antona & Mazzitelli (1990).

4.1. Atmospheres, Spectra, and Colors

In order to properly identify and characterize white dwarfs, we need to understand their appearance. Thus, accurate modeling of the radiative transfer in the outer layers of the star is a necessity. Cool white dwarfs have convection zones that extend very close to the surface (Fontaine & Van Horn 1976, Böhm et al. 1977, Bergeron, Wesemael & Fontaine 1992), which serves to regulate the heat transfer from the interior to the atmosphere as well as to mix atmospheric constituents with material (carbon and possibly oxygen) dredged up from deeper in the star. Also important is the contribution from various opacity sources that come into play once the atmospheric materials recombine. At low temperatures, the opacity of pure hydrogen and pure helium differ dramatically because of the propensity of the former to form molecules. As we have seen, the collisionally induced absorption

(CIA) of molecular hydrogen becomes progressively more important as white dwarfs cool to $T_{eff} \sim 4000$ K (Bergeron, Saumon & Wesemael 1995). Not only does the increased opacity slow the cooling rate, but, as we have seen, the strong wavelength dependance also has a dramatic effect on the colors (Hansen 1998, Saumon & Jacobsen 1999) and spectral appearance (Bergeron, Saumon & Wesemael 1995, Hansen 1999a, Bergeron 2001, Bergeron & Leggett 2002), leading to the depression of flux in the infrared and then red wavelengths.

At hotter temperatures the spectral energy distributions of hydrogen atmosphere dwarfs led Bergeron, Ruiz & Leggett (1997) and Bergeron, Leggett & Ruiz (2001) to infer that there is probably an opacity source missing from the models, which affects primarily the shorter wavelengths. In particular, for the fits to pure-H atmospheres, the broad band B photometric passband is systematically weaker than the models for the coolest objects. (Hence, B is not used in their fits.) Wolff, Koester & Liebert (2002) show that even more dramatic observational deficiencies with respect to model predictions exist in *HST* ultraviolet fluxes observed for three cool white dwarfs of types DA, DZ, and DQpec. The most likely candidates for this missing opacity are (*a*) some kind of pseudo-continuum opacity operative at short wavelengths, most likely due to the Lyman edge (Bergeron, Leggett & Ruiz 2001), and/or (*b*) incorrect treatment of the red wing of Lyα at wavelengths far from the line center (Wolff, Koester & Liebert 2002).

The large difference between hydrogen and helium atmospheres at low temperatures also lends importance to the possibility of mixed hydrogen and helium atmospheres. The CIA opacity relies on the perturbation of the H_2 molecule by a neighboring atom or molecule to provide a temporary dipole moment, which allows the absorption of light. Thus, helium atoms can also provide a contribution to the CIA opacity by H_2–He collisions (Borysow et al. 1997), leading to a significant and generally stronger infrared absorption for mixed H-He atmospheres. Even in the absence of hydrogen a trace amount of heavier material can contribute electrons to provide He$^-$ opacity in the otherwise extremely transparent helium atmosphere (Bergeron, Saumon & Wesemael 1995, Jorgensen et al. 2000). Thus, the possibility of accretion of interstellar or circumstellar material, and the possible influence on the atmosphere and cooling, must be carefully considered. In cool helium atmospheres, and potentially also in cool hydrogen atmospheres (although to a lesser extent) the opacities can also be reduced by the collective interactions between atoms at the high densities that exist at the photosphere (Iglesias, Rogers & Saumon 2002).

As the star cools, the decreasing opacity of the atmosphere causes the position of the photosphere to move toward higher surface pressure (inward), as shown in Figure 10 for an atmosphere assumed to be pure-H. The change in the photospheric pressure, by several orders of magnitude, has a big effect on the cooling models, as discussed in Section 4.5.

We note that the mass above the photosphere is roughly

$$M_{atm} = 4\pi R^2/\langle\kappa\rangle \sim 6 \times 10^{-15} \, M_\odot R_9^2/\langle\kappa\rangle, \tag{1}$$

where R_9 is the radius in 10^9 cm and $\langle\kappa\rangle$ is the mean opacity in the atmosphere. Thus, for a hydrogen atmosphere it increases from $\sim 10^{-15} \, M_\odot$ to $\sim 10^{-12} \, M_\odot$ as the
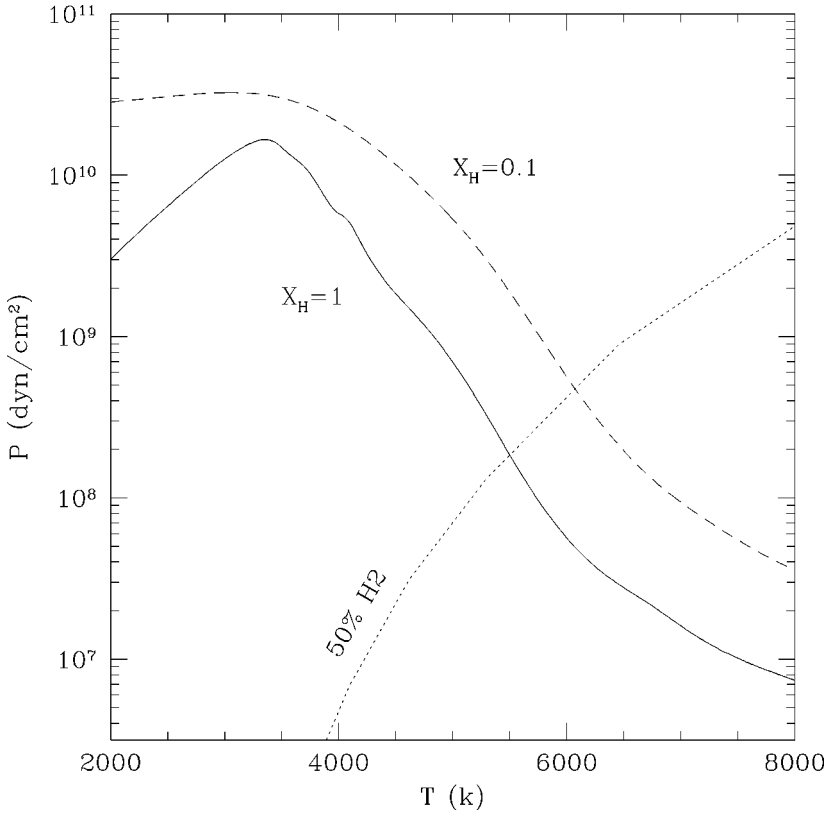
Figure 10 The solid line shows the temporal evolution of the Rosseland photosphere for a pure hydrogen, $\log g = 8$ atmosphere. The dashed line shows the equivalent for an atmosphere 10% hydrogen and 90% helium by mass. The dotted line shows the line for $X_{H_2} = 0.5$ (in the pure hydrogen case).

star cools, and for a pure helium atmosphere $\sim 10^{-14}\ M_\odot$ to $\sim 10^{-9}\ M_\odot$ (assuming no other source of opacity). Thus, at average interstellar medium (ISM) accretion rates (see Section 4.3), it takes only 10^3–10^5 years to accrete a photosphere's worth of material. This would greatly change the spectrum were it not for dilution into a much more massive convective envelope.

4.2. The Convection Zone

The outer convection zone of a cool white dwarf plays a vital role in both regulating the heat transfer through the envelope and mixing the material in the outer layers, including any heavy elements accreted from the external environment (DZ, DAZ stars), and/or carbon (and potentially oxygen) dredged up from the diffusion tail of the core. For a hydrogen atmosphere star, the convection zone begins to form at $T_{eff} \sim 15,000$ K. The region of parameter space associated with DA white

dwarf pulsations, the ZZ Ceti strip, is associated with this epoch when the sur-
face convection zone is small. As the star continues to cool, the convection zone
advances inward to greater depths (Fontaine & Van Horn 1976) and eventually
bottoms out when the base reaches the edge of the degenerate layer. Interior to this
point, the energy transport is dominated by electron conduction, which is more ef-
ficient than convection and therefore prevents the convection zone from advancing
further inward. In fact, once the convection zone has bottomed out, it will begin
to retreat once more towards the surface as the degenerate core continues to grow.
The convective region may be defined by the Schwarzschild criterion

$$\frac{1}{\kappa} \frac{T^4}{P^4} \frac{\partial \ln T}{\partial \ln P} < \frac{3}{64\pi G\sigma} \frac{L}{M}, \tag{2}$$

where L/M is a constant in the plane parallel surface approximation appropriate to
white dwarfs (L/M $\sim 10^{-3}$–10^{-5} by the time white dwarfs become convective).
Figure 11 shows the part of the parameter space that is convective for white dwarfs.
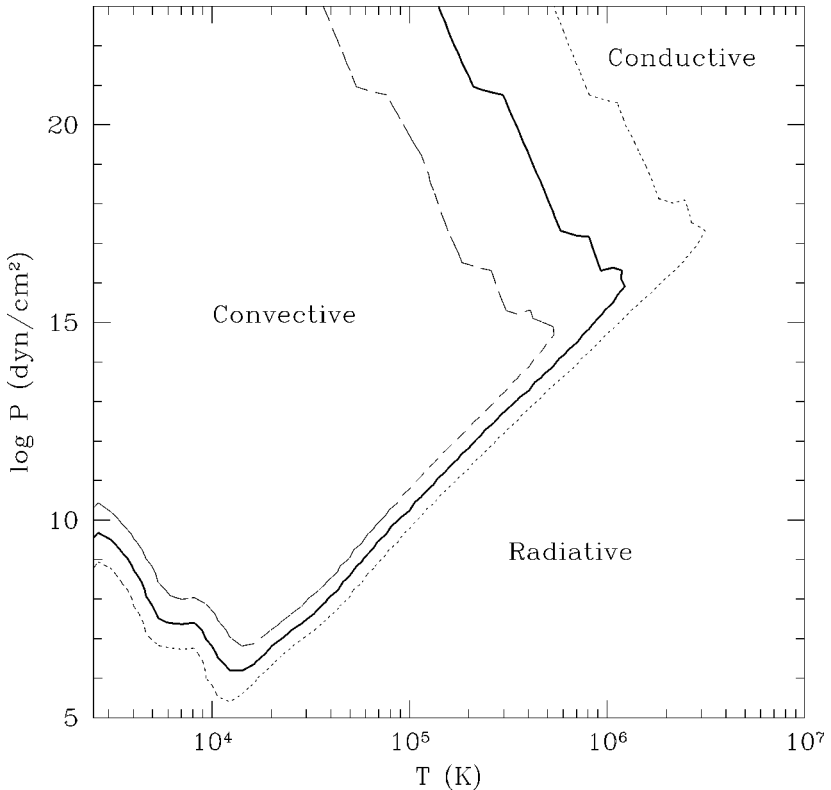
Figure 11   The heavy solid line delineates the convective region in the case L/M =
10^{-4}. The dotted and dashed lines correspond to 10^{-3} and 10^{-5}, respectively.

The slow encroachment of the conductive degenerate region onto the convection zone is evident at the top of the diagram.

The epoch at which the convection zone reaches the degenerate core is an important one, as it results in the disappearance of the radiative buffer zone that previously existed between the outer convective region and the inner degenerate region. The lack of this buffer zone means that there is therefore a very strong coupling between the surface temperature and the core temperature (Fontaine & Van Horn 1976, D'Antona & Mazzitelli 1990, Hansen 1999a, Fontaine, Brassard & Bergeron 2001). The strong coupling results from the fact that the degenerate core is essentially isothermal and the temperature gradient in the convection zone is set by the adiabatic gradient. The direct connection between these two regions fixes the central temperature as a function of surface temperature. The net result is that the cooling becomes quite sensitive to the treatment of the outer boundary condition. This realization has spurred the recent move to comprehensive models of the coupling between atmospheric models and interior models (Hansen 1998, 1999a; Salaris et al. 2000; Fontaine, Brassard & Bergeron 2001).

This strong coupling also happens to occur during the same epoch when the atmospheric parameters are changing quite dramatically as a result of the recombination of the atmospheric material and the consequent large changes in the atmospheric opacity and photosphere location.

4.3. Chemical Evolution

The demonstration that an individual cool white dwarf can change its chemical evolution as it evolves (Bergeron, Ruiz & Leggett 1997) requires an explanation for how hydrogen and helium can appear and disappear in the same star at different epochs. Obvious components of this story are accretion and convective mixing between the atmospheric layers and deeper zones within the star. However, exactly how these pieces fit together remains a largely unsolved jigsaw puzzle.

Bergeron, Ruiz & Leggett (1997) produced the following straw-man model to explain the observed "non-DA gap" between 5000 to 6000 K. They consider a pure helium atmosphere dwarf that accretes hydrogen from the interstellar medium. For neutral material, hydrogen has a considerably larger opacity than helium (due first to the H^- opacity and then later the formation of H_2 molecules), and even a small amount should dramatically effect the surface conditions. However, if hydrogen is slowly added into the dense conditions appropriate to a pure helium atmosphere, Bergeron, Ruiz & Leggett (1997) hypothesized that the hydrogen atomic levels would be quenched by pressure ionization and the H^- bound level destroyed. This mechanism would imply a much larger hydrogen fraction is needed before the opacity were raised to the point where the star would show a hydrogen atmosphere. Such a mechanism would explain the blue edge of the non-DA gap and the sudden appearance of hydrogen in the atmospheres at cooler temperatures. The red edge, and the re-appearance of helium in some stars, would then be the consequence of the continuing increase of the convection zone mass and the consequent dilution of the hydrogen with an ever increasing amount of helium.

Malo, Wesemael & Bergeron (1999) investigated this promising idea but found that it failed because even if the H$^-$ bound level is destroyed, the free electrons from the pressure ionized hydrogen provide enough opacity to have a significant effect once $N_H/N_{He} > 10^{-6}$. For an assumed interstellar gas density (n) of 1 cm^{-3}, the approximate accretion rate of a disk star moving with velocity V through the medium is (Bondi & Hoyle 1944)

$$\dot{M} \sim \pi \frac{(GM)^2 \rho}{V^3} \sim 10^{-17} \, M_\odot \cdot yr^{-1} \left(\frac{V}{30 \, km \cdot s^{-1}} \right)^{-3} n, \qquad (3)$$

and the convective zone mass $\sim 10^{-4} \, M_\odot$, so that only $\sim 10^7$ years is required to accrete enough hydrogen, much less than the cooling time to $T_{eff} \sim 5000$–6000 K. For a pure hydrogen envelope, see Figure 12; for a helium boundary condition, see Figure 13.

Hansen (1999a) noted that the increased rate of cooling of white dwarfs with pure helium atmospheres may contribute to the non-DA gap by separating white dwarfs of similar age in terms of effective temperature. However, this cannot be the complete explanation because the non-DA gap is prefigured by compositional anomalies in white dwarfs with effective temperatures slightly above 6000 K (Bergeron, Leggett & Ruiz (2001). As noted earlier, these authors found that DQ stars are not found below 6400 K, but stars showing C_2H in their spectra are found, suggesting that this class of stars also shows an increased amount of atmospheric hydrogen at cool temperatures. The exact interplay between accretion and convective mixing that gives rise to these changing abundances remains poorly understood.

It has been argued that hot white dwarfs, especially if they are rotating modestly and possess even a weak magnetic field, may inhibit accretion from ambient interstellar gas because they can ionize this gas and deflect it—the Illarionov & Sunyaev (1975) "propeller mechanism," discussed in the context of white dwarfs by Wesemael & Truran (1982). Whether this works for hot white dwarfs or not (and there are heavy elements and hydrogen detected in some hot white dwarfs), it is hard to imagine that accretion doesn't occur at least when a cool star, which cannot ionize the gas and dust, passes by chance through a gas cloud. However, the above formula assumes a steady rate, which might be an average if the actual rate is highly variable.

Figure 13 compares the mass of the convection zone and photosphere of a pure helium atmosphere white dwarf to the amount of hydrogen accreted at the rate (3) from the ISM over the course of the white dwarf age. Upon striking the surface, it becomes diluted into the massive convective envelope. At the 15,000 K temperature at the left edge of the plot, a predicted n(H)/n(He) ratio of 10^{-3} to 10^{-4} is consistent with the observed trace detections of H in DBA white dwarfs and at least $\sim 20\%$ of DB white dwarfs (Shipman, Liebert & Green 1987). At hotter temperatures, the convection zone grows in mass to perhaps keep pace with the amount accreted. As the atmosphere cools, however, and any atmospheric hydrogen recombines, trace amounts of hydrogen become harder to detect. Nonetheless, we noted earlier that
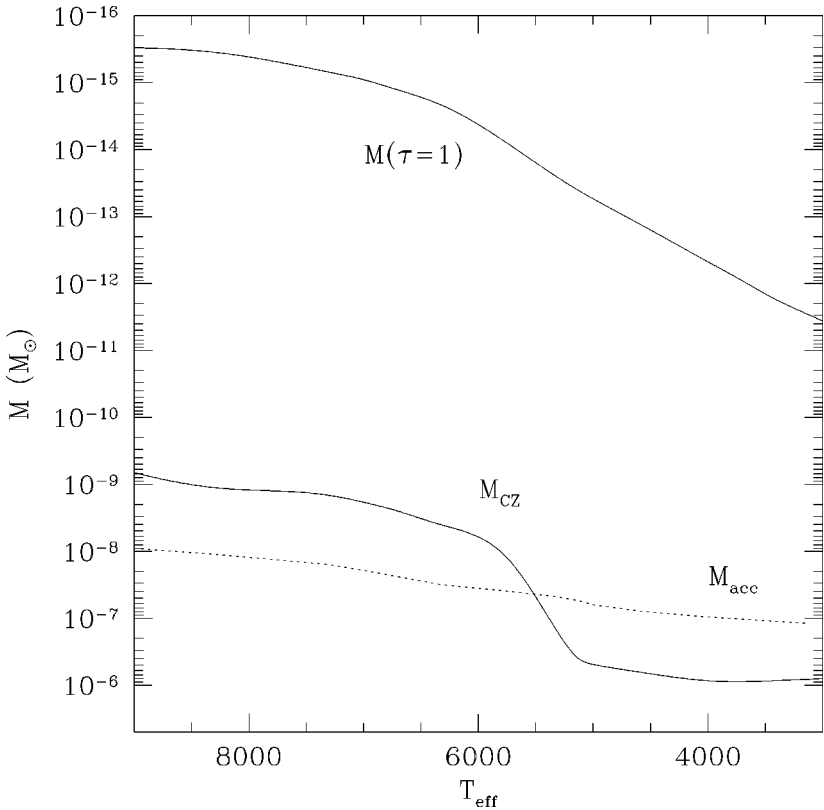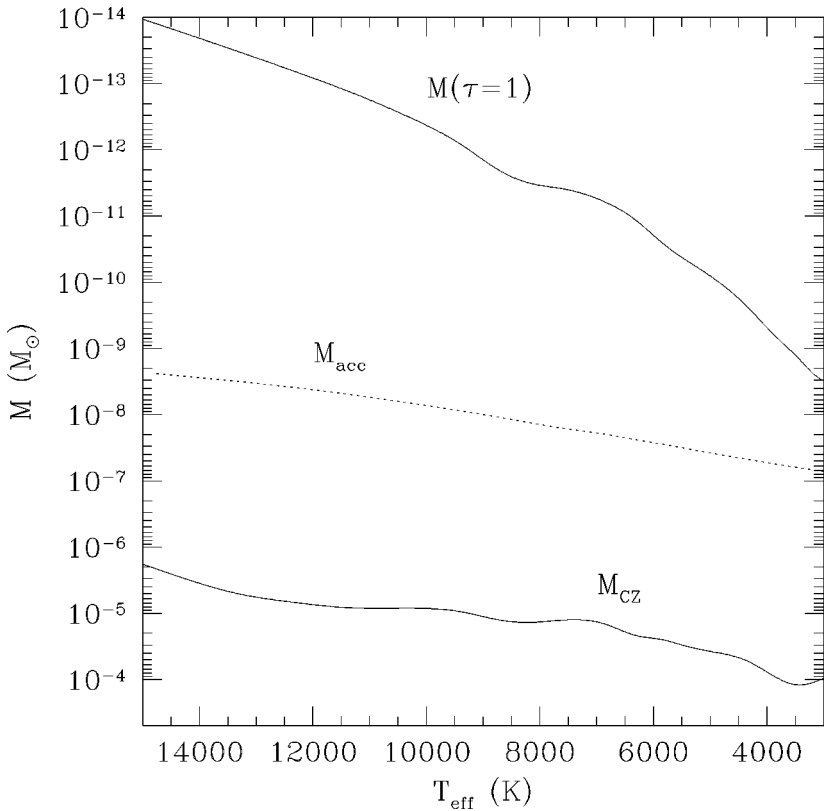
Figure 12   The upper solid line shows the evolution of the photospheric mass with
time for a 0.6 $M_\odot$ white dwarf with a pure hydrogen atmosphere. The lower solid line
indicates the total mass contained in the convection zone. The dotted line indicates the
mass accreted at a constant rate of $\dot{M} = 10^{-17}\ M_\odot \cdot year^{-1}$. The sharp increase in the
mass of the convection zone between 5000 and 6000 K is halted at lower temperatures
as the convection zone approaches the degenerate layer.

a minority of cool stars showing H lines fit He-rich atmospheres, and most of these
show metals (DZA). The convection zone begins to recede when it couples with
the degenerate core, which itself is expanding outward in mass. As the convective
region recedes in mass, the increasing mass of hydrogen may now get easier to
detect. If one took the calculation of the pure-He case shown in Figure 13 literally,
this might happen just below a T_{eff} of 4,000 K. Such a scenario provides a natural
explanation for the existence of very cool disk white dwarfs that show H_2 CIA
absorption but with mixed or very He-rich atmospheric compositions. This is
exactly what is required in the analyses of the few of these objects (Harris et al.
1999, Bergeron 2001, Oppenheimer et al. 2001b, Bergeron & Leggett 2002), as
suggested by these last authors.

Figure 13 The upper solid line shows the evolution of the photospheric mass with time, for a 0.6 $M_\odot$ white dwarf with a pure Helium atmosphere. The lower solid line indicates the total mass contained in the convection zone and the dotted line indicates the mass accreted at a constant rate of $\dot{M} = 10^{-17}\ M_\odot \cdot \mathrm{year}^{-1}$. It is evident that both the photospheric mass and the convection zone mass are considerably larger than for the case of a hydrogen atmosphere. This represents the most extreme case because as hydrogen is accreted, the increase opacity will decrease the photospheric and convection zone masses.

The above scenario has a big caveat. While the model rightly begins with a pure-He composition, the accumulation of hydrogen would add a much stronger opacity source, which would have significant effect on the atmospheric boundary condition and would, in turn, alter the envelope structure and the depth of the convection zone. Thus, we may be guided by the studies of the carbon dredge-up of DQ stars by Pelletier et al. (1986). The observed abundance of carbon appears to be highest near $T_{\mathrm{eff}} \sim 10,000$ K, for an assumed q_{He} of 10^{-3} to 10^{-4}. While this calculation should be redone with updated physics, the convective layer

probably reaches maximum mass at a warmer T_{eff}. The actual envelope structures for He-rich white dwarfs probably lie between the two extremes of Figure 12 and Figure 13.

Note that it has usually been assumed in the literature that the accretion is from the ISM, either steadily at a very low rate, or primarily when the star happens to pass through a gas cloud in its galactic orbit. Strong support for this hypothesis is espoused in the series of papers by Dupuis, Fontaine & Wesemael (1993) and references therein. These authors argue that, although using a simplified picture of the ISM, the observed metal abundance patterns are accounted for within this framework. For many individual stars it is also possible to infer the direction of motion necessary for the accretion rates to maintain the photospheric metal abundances, rates that agree remarkably well with the estimates for denser patches of the ISM. However, Aannestad et al. (1993) argue with equal conviction that this picture is not correct. The cool DZ stars have massive helium convection zones, and these authors argue that the accretion rates cannot be high enough to produce the derived abundances of the heavy elements given the absence of dense gas clouds in the solar neighborhood. They argue also that the positions of DZ stars show no correlation with the locations of the known local clouds. Moreover, the average gas density in this warm, low-density region is only a fraction of the 1 cm^{-3} assumed in our straw-man calculation of the accretion rate. Hence, we have made an assumption in the preceding, speculative paragraphs that is controversial.

Another possible origin for the "accretion," at least for the DAZ stars with shallower envelopes, are impacts from comets from the star's Oort cloud, which might have survived its prior evolution (Alcock, Fristrom & Siegelman 1986). Zuckerman & Reid (1998) concluded from earlier studies of DAZ that their data set were not easily reconciled with either the comet or ISM accretion models. However, G 29-38 is a DAZ star not only showing an unusual multimetal spectrum of Ca, Mg, and Fe at ultraviolet and optical wavelengths, it has long been known to exhibit an infrared excess from the near JHK bands (Zuckerman & Becklin 1987) to 10 μm (Tokunaga, Becklin & Zuckerman 1990). The latter authors argued that the star was enveloped in particulate matter, which in turn its photons were exciting. Presumably, this is the source of the metals detected at the photosphere, and it is difficult to envision the mass of the enshrouding dust being consistent with a finite number of disrupted comets. However, G 29–38 appears to be unique among the ~120 DA stars studied in a recently-completed investigation (Zuckerman et al. 2003). Excluding the 17 stars in moderately close DA + dM binaries, about 25% of the remainder show Ca II absorption in high resolution, high signal-to-noise ratio spectra obtained with the HIRES echelle spectrograph at the Keck I telescope. They are still having difficulty reconciling these extensive observations with any model. This means that the fraction of known cool DA stars showing heavy elements is higher than for non-DA stars. However, few cool non-DA stars have been studied at the relevant 3900–4000 Å wavelengths with such precision.

4.4. Core Composition

The treatment of the atmosphere determines how the heat flow from interior to exterior is regulated. The other important aspect of the cooling model is how much energy there is to be radiated. Thus, a treatment of the degenerate core, specifically the evolution of the heat capacity, is important.

The heat capacity of the electrons is negligible, as only that fraction near the surface of the Fermi sea can contribute significantly. The heat capacity of a white dwarf is dominated by the ions in the core, which are not degenerate. However, as the white dwarf cools, the Coulomb interaction between neighboring ions continues to increase. These interactions lead to short range order, increasing heat capacity and eventually leading to crystallization, with the concomitant release of latent heat (Lamb & Van Horn 1975) and change in the heat capacity. The transition to the solid phase is found to occur at a value of the critical Coulomb parameter

$$\Gamma = \frac{(Ze)^2}{rkT} = 170\text{–}200 \tag{4}$$

(Ichimaru, Iyetomi & Ogata 1988; Stringfellow, De Witt & Slattery 1990; Segretain & Chabrier 1993) where Z, r are the atomic charge and interatomic separation respectively. Once the core has crystallized, the heat capacity drops $\propto T^3$ (the Debye regime) as fewer and fewer of the crystals oscillation modes are excited. This leads to rapid cooling at late times for crystallized white dwarfs.

At the high densities appropriate to white dwarf interiors, it is not only the Coulomb interaction that is important, but also the corrections to the free energy that arise from the quantum nature of the interactions. Chabrier, Ashcroft & DeWitt (1992) demonstrated that although the average interionic spacing is smaller than the ion De Broglie wavelength near the classical crystallization point, the rms fluctuations about the mean ion positions are dominated by quantum zero-point oscillations, rather than the classical thermal kinetic energy. More specifically, the ratio of ionic plasma frequency (ω_p) to the equivalent classical thermal quantity is

$$\frac{h\omega_p}{kT} = 4 \times 10^3 \frac{\rho^{1/2}}{T} = 2 \left(\frac{\Gamma}{200} \right) \left(\frac{\rho}{10^6 \text{ g} \cdot \text{cm}^{-3}} \right)^{1/6}. \tag{5}$$

Thus, the classical crystallization boundary lies in the regime of parameter space where quantum effects are already dominant. A more detailed calculation of the fluid-solid transition by Chabrier (1993), using a model for the quantum solid and an empirical Lindemann criterion, finds that the location of the fluid-solid transition remains largely unchanged by these considerations. However, that is not to say that the quantum corrections are irrelevant. Indeed, the fact that quantum effects are important before crystallization raises the possibility that the white dwarf enters the Debye regime before crystallization begins (Chabrier 1993), although the extent of this correction depends on the degree to which short-range order contributes to the heat capacity in the liquid phase.

The nuclear burning history of the progenitor imprints a particular chemical composition profile on the white dwarf core. The first calculations of the

crystallization of a carbon oxygen mixture (Shaviv & Kovetz 1976) assumed that the solid and liquid compositions were the same. Stevenson (1980) analyzed the carbon/oxygen phase diagram and found it to be of the eutectic type, i.e., the solid phase composition could be considerably more oxygen-rich than the liquid phase. Subsequent analyses have found alternative forms for the phase diagram, from spindle (Barrat, Hansen & Mochkovitch 1988; Segretain & Chabrier 1993) to azeotropic (Ichimaru, Iyetomi & Ogata 1988). The importance of this is that the compositional separation at crystallization can lead to a rearrangement of the internal density profile and a consequent release of binding energy in the form of heat (Garcia-Berro et al. 1988, Isern et al. 1991, Segretain et al. 1994). This results in a temporary slowing of the cooling and may influence the disk luminosity function (Hernanz et al. 1994). The size of the delay ranges somewhat between different calculations depending on whether the white dwarf core is stratified in the progenitor stages (Salaris et al. 1997), the treatment of the outer boundary condition (Hansen 1999a, Isern et al. 2000), or the treatment of the phase diagram and mixing in the liquid phase (Mochkovitch 1983, Montgomery et al. 1999, Bildsten & Hall 2001). The contribution of trace amounts of denser species may also have an effect for very massive white dwarfs (Segretain et al. 1994) although the effect is much reduced when a true three-body phase diagram is used (Segretain 1996) for the carbon/oxygen/neon instead of an effective two-body nitrogen/neon treatment.

4.5. Cooling Curves

The review of D'Antona & Mazzitelli (1990) marks a transition in the calculation of white dwarf cooling models from studies of physical processes (Lamb & Van Horn 1975, Iben & Tutukov 1984b, Koester & Schönberner 1986, D'Antona & Mazzitelli 1989) to detailed applications of suites of models to extract information about the underlying population (Winget et al. 1987, Wood 1992, Hernanz et al. 1994, Hansen 1999a, Chabrier et al. 2000, Salaris et al. 2000). The overall qualitative picture of white dwarf cooling remains intact, and the work over the past decade has focused on obtaining more quantitative estimates of white dwarf ages and the underlying theoretical uncertainties.

A popular method for computing simple white dwarf models has been to treat the core and envelope structures separately. Many groups (e.g., Segretain et al. 1994, Hernanz et al. 1994, Salaris et al. 1997, Chabrier et al. 2000) use the fact that the core temperature is roughly isothermal to simplify the calculation by assuming simple luminosity–core temperature ($L - T_c$) relations obtained from more detailed models and treating only the core in detail. While this allows for a convenient treatment of separation effects, it is not a fully self-consistent solution and is at the mercy of the quality of the assumed $L - T_c$ relation.

Cooling models based on a full Henyey treatment have been calculated by Wood (1992, 1995); Hansen (1999a); Benvenuto & Althaus (1999); Salaris et al. (2000); and Fontaine, Brassard & Bergeron (2001). These treat the core-envelope coupling in a consistent manner but don't always treat the outer boundary condition in a

manner consistent with the properties determined from detailed atmospheric models, such as those in Bergeron, Saumon & Wesemael (1995). Earlier models used simple gray atmosphere calculations to determine the boundary conditions, and used only approximate opacities for the helium-dominated cases. In recent years, several groups have incorporated accurate atmosphere models in the calculation of the outer boundary conditions, leading to fully self-consistent atmosphere and interior calculations (Hansen 1998, 1999a; Salaris et al. 2000; Fontaine, Brassard & Bergeron 2001). Detailed models of this type are important because much of the cooling evolution described below is driven by the changes in the outer boundary condition driven by the changing atmospheric opacity.

Figure 14 shows a comparison of two cooling models, with 0.6 $M_\odot$ and 0.9 $M_\odot$, respectively. The models are for pure carbon cores and hydrogen atmosphere
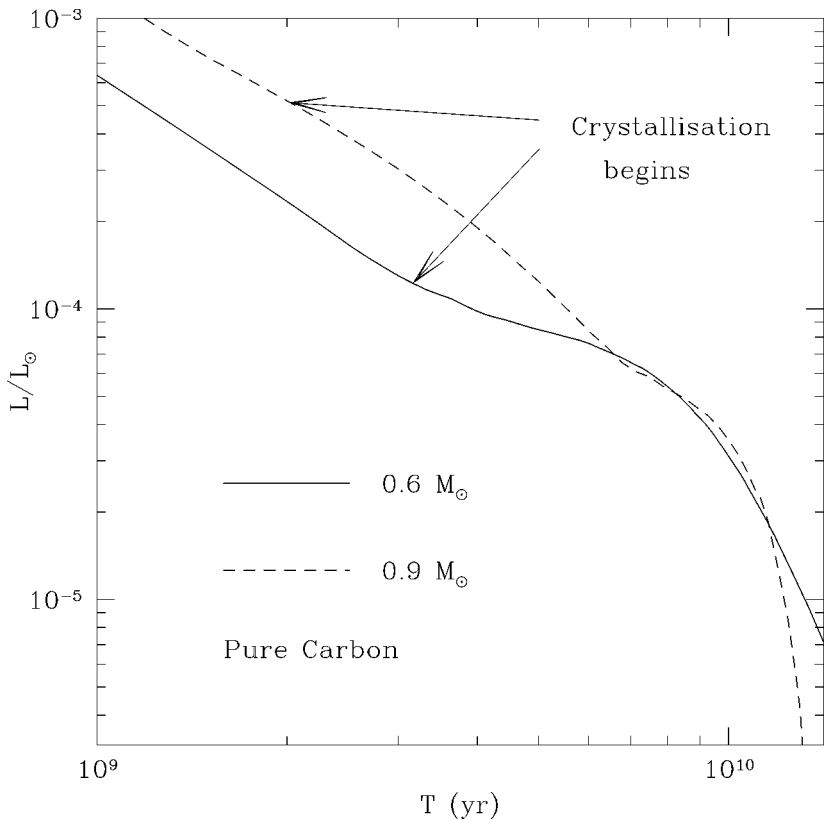
Figure 14 The solid and dashed curves show the cooling of 0.6 and 0.9 $M_\odot$ models, respectively, both with pure carbon cores. The location of the onset of core crystallization is shown. The more massive star is brighter at early times but eventually becomes fainter once it has entered the Debye cooling regime.

boundary conditions (Hansen 1999a). At early times, the more massive white
dwarf is brighter, as befitting its greater heat capacity. However, massive white
dwarfs have higher central densities and begin to crystallize first. Once they enter
the Debye regime in which the heat capacity drops (because not all the quantum
vibrational states of the crystal lattice are excited at low temperatures), the massive
white dwarfs cool faster, so that the cooling curves cross at $\log L/L_{\odot} \sim -4.2$.
At roughly the same luminosity, the cooling curves for white dwarfs of mass 0.5–
0.9 $M_{\odot}$ flatten out. This is due, in part, to the release of the latent heat of crystal-
lization, but the majority of the effect is actually driven by the change in the outer
boundary condition. Once the convection zone has advanced inward to the point
where it couples directly to the interior degenerate layer (Section 4.2), the changes
in the atmospheric temperature and pressure couple directly to changes in the cen-
tral temperature, effectively imposing a monotonic relation $T_c = T_c(T_{eff})$. When
the atmospheric constituents recombine and then form molecules, the average at-
mospheric opacity drops, causing the photosphere to move to higher pressures
(Figure 10). This results in a steepening of the slope dT_c/dT_{eff}, and thus the star
spends more time at this luminosity and effective temperature because it has to
radiate more energy (corresponding to the larger ΔT_c per unit ΔT_{eff}) in order to
cool to lower T_{eff}.

Figure 15 demonstrates how these various effects are expected to manifest
themselves within the observed sample. The points are the white dwarfs drawn
from Leggett, Ruiz & Bergeron (1998) and the proper motion complete sample of
Leggett, Dahn & Monet (1988). Solid points indicate hydrogen atmospheres and
open points indicate helium-dominated atmospheres. Those for which a gravity
has been assumed rather than measured are shown at $\log g = 8$ with no error bar on
$\log g$. The data are compared to a suite of models for carbon/oxygen cores, drawn
from Hansen (1999a). The dashed and solid lines represent two sets of isochrones
based on these models. The dashed lines indicate white dwarf ages only (in gi-
gayears). The solid lines include an estimate of the progenitor main sequence
lifetime based on the main sequence-white dwarf relation detailed in model C of
Table 2 in Wood (1992). For white dwarfs $M < 0.6 \, M_{\odot}$, the progenitor age is
significant, and, given the uncertainty in the mass sequence-white dwarf relation,
we have set the progenitor age for all $M < 0.6 \, M_{\odot}$ white dwarfs equal to 2.3 Gyr.
This diagram also displays several of the features referred to in Section 4.3. In
particular, the non-DA gap is seen in the predominance of hydrogen atmosphere
dwarfs between 5000 and 6000 K. The atmospheric heterogeneity of the sample
above and below this range is also evident.

Figure 16 shows the same data, but now compared to internal milestones of the
models themselves. The solid line indicates the classical crystallization boundary
$\Gamma = 175$. The long dashed line indicates the boundary $\eta = E_0/kT = 5$, where E_0
is the ionic zero-point energy, illustrating the importance of quantum effects in the
ionic fluid well before the classical crystallization boundary (Chabrier, Ashcroft
& De Witt 1990; Chabrier 1993). The short dashed line indicates the boundary
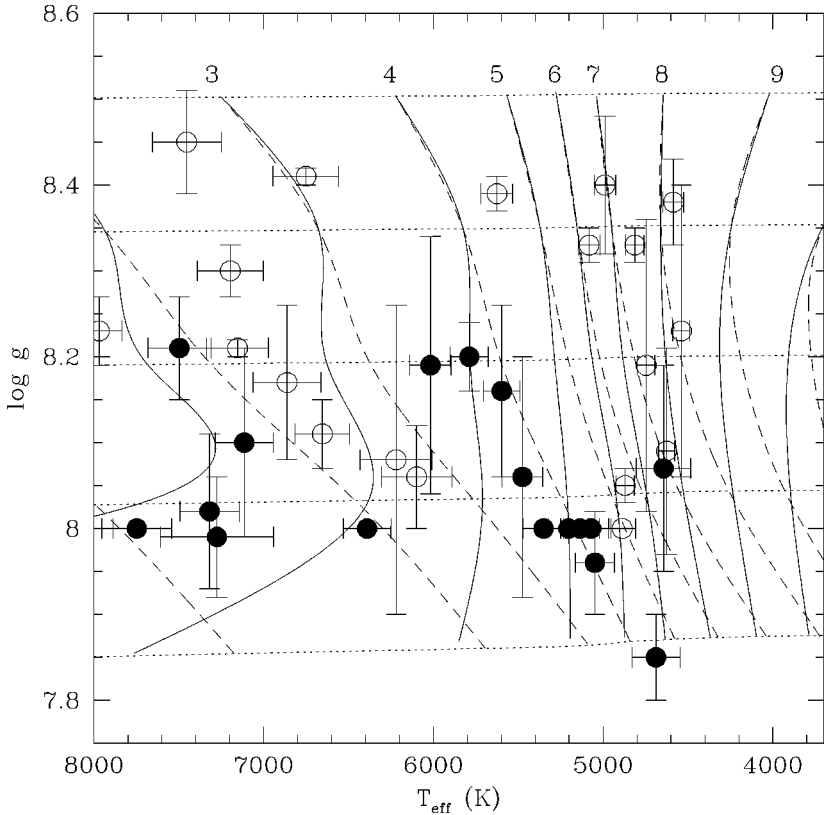where the base of the convection zone penetrates below $\log P = 15$. As can be seen

Figure 15 Observational data compared with model isochrones. The solid points indicate hydrogen atmospheres and the open points are helium dominated atmospheres. The dotted lines are for 0.5–0.9 $M_\odot$ models, with hydrogen atmospheres, labeled from the bottom. The dashed curves are isochrones (white dwarf age only) labeled in Gyr, whereas the solid curves are isochrones including a model for the progenitor lifetime (as discussed in the text). One very massive white dwarf lies above the region shown, and several low-mass white dwarfs (presumably the result of binary evolution) fall below the region shown.

from Figure 12, the convection zone mass increases sharply once the boundary condition begins to change in response to the decreasing atmospheric opacity. The criterion $\log P = 15$ marks the approximate transition where the rapid increase in the convection zone mass changes to a slower growth. The slower cooling that results, combined with the release of latent heat, is probably responsible for the observed distribution of stars in this diagram. However, the reader is cautioned that this diagram is only illustrative because the individual objects are not weighted by their relative detectabilities.
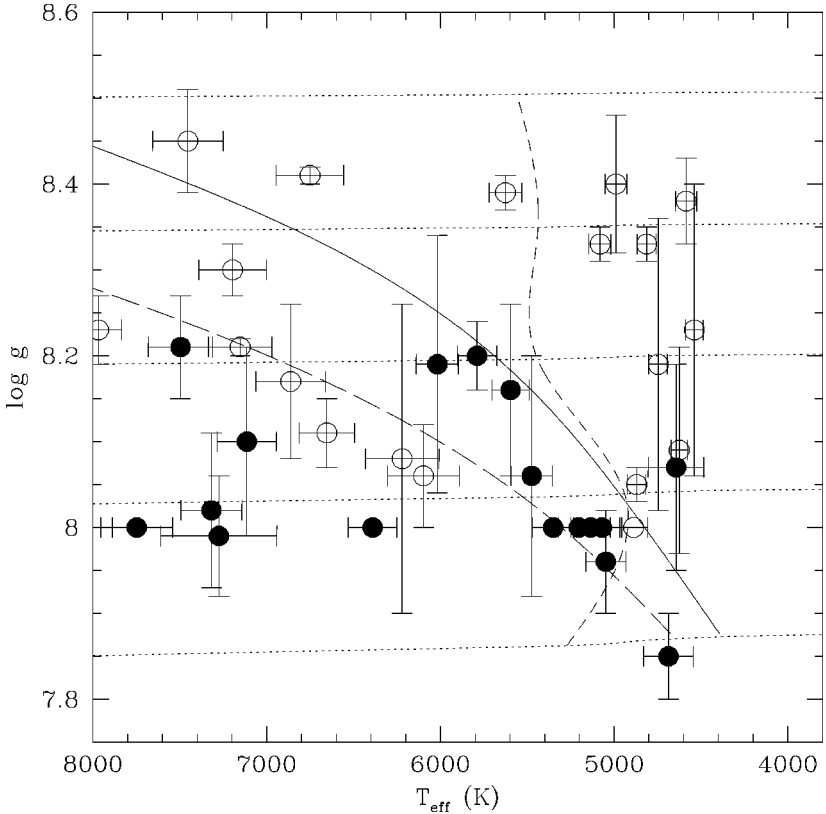
Figure 16   The observed points are as before. The solid line indicates the classical crystallization boundary. The long dashed line indicates a line of constant ion degeneracy $\eta = 5$. The short dashed line shows where the convection zone penetrates below a layer $\log P = 15$ and denotes the approximate location of the end of the rapid inward motion of the convection zone. Note that this is not the maximum extent of the convection zone, which occurs at cooler effective temperatures.

The internal structure is also of interest. Figure 17 shows the evolution of the thermal profile of a 0.6 $M_\odot$ white dwarf. The short and long dashed lines indicate the crystallization boundary and ion degeneracy boundary, respectively. The dotted line indicates the base of the convection zone.

The above illustrative figures have drawn from a single set of cooling models. Full consideration of the uncertainties in our understanding of white dwarf cooling must incorporate a comparison between different models. To that end, Figure 18 shows the comparison of cooling curves from three different calculations in the literature for a roughly standard model of 0.6 $M_\odot$, with a carbon/oxygen core, and helium and hydrogen mass fractions of 10^{-2} and 10^{-4}, respectively. The
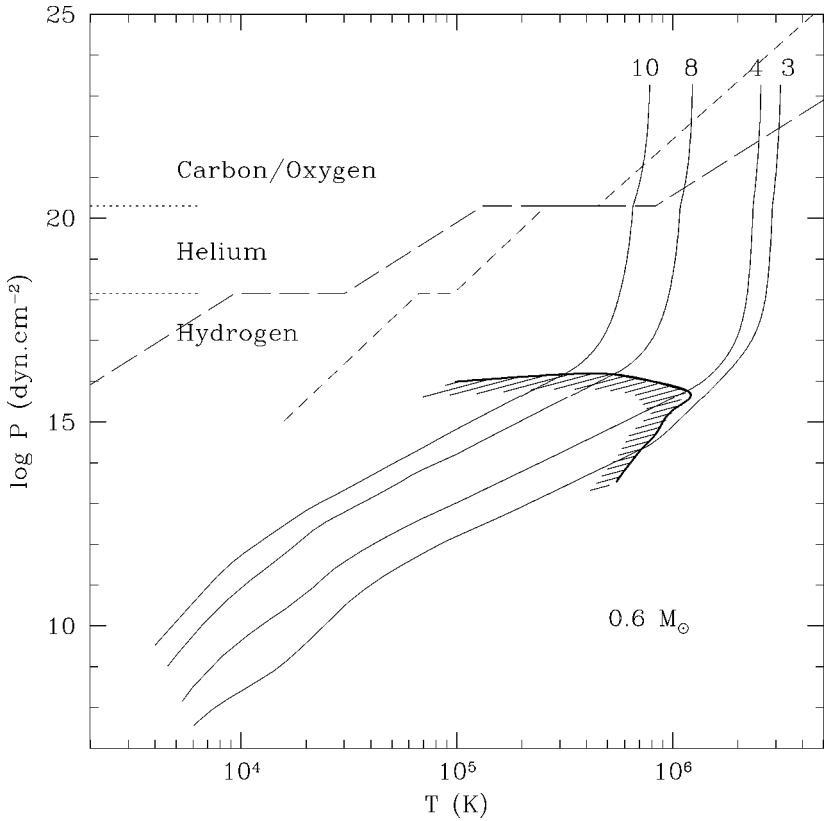
Figure 17   The solid curves are the thermal profiles of a 0.6 $M_\odot$ white dwarf at 3, 4, 8, and 10 Gyr, respectively. By 10 Gyr, the entire carbon/oxygen core has crystallized and the convection zone has reached its maximum depth and begun to retreat. The short dashed line indicates the crystallization boundary, the jumps being due to the change in chemical composition between layers. The long dashed line is the ionic degeneracy boundary $\eta = 1$. Note that this is not to be confused with the electron degeneracy boundary, which extends to much lower pressures. The shaded boundary indicates the base of the convection zone.

only entirely independent calculation in this group is that of Hansen (1999a). The calculations of Salaris et al. (2000); Chabrier et al. (2001); and Fontaine, Brassard & Bergeron (2001) use different internal models, but the outer boundary conditions are drawn from the same atmosphere models. Fontaine, Brassard & Bergeron (2001) did not include any tables. The points are thus read off of curve 2 in Figure 7 of that paper. The qualitative agreement in all the curves is encouraging, although there remain quantitative disagreements at the 10% level, which require further work to resolve. Potential contributing factors include differences in the
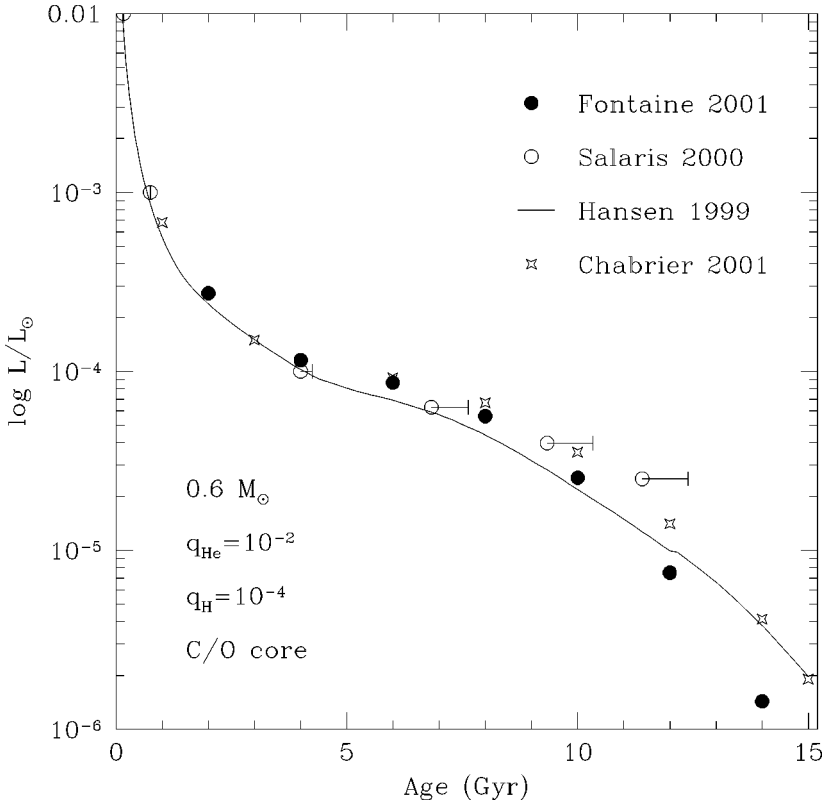
Figure 18 The solid curve shows the cooling of a 0.6 $M_\odot$ model from Hansen (1999). The open points are from Salaris et al. (2000), for a 0.61 $M_\odot$, fully consistent model. The filled points are from Fontaine et al. (2001). The open stars points are from Chabrier et al. (2001), which, while still not a fully self-consistent code, at least uses $L - T_c$ relations based on nongray atmosphere models, and so should be more accurate than previous calculations in this vein. The extensions of the Salaris points indicate the extra delay in the cooling if they take into account the release of separation energy upon crystallization.

treatment of core composition (particularly the treatment of separation energy upon crystallization) and nonideal effects of the equation of state in the atmosphere.

5. SUMMARY

Over the past decade, the study of old white dwarfs has advanced on several fronts. In addition to the white dwarfs of the galactic disk, we have examples of white dwarfs from the thick disk and almost certainly the halo as well. The detection

of white dwarfs in globular clusters promises to open a window on the very early history of our Galaxy. We have also made significant progress in examining the physical properties of white dwarfs on the theoretical and observational side. As is usually the case, advances have also posed new questions. The diversity of spectral properites, and their evolution as a function of temperature, pose an outstanding challenge to the theory. The division of white dwarfs into different kinematic populations remains somewhat uncertain because of the relatively poorly understood normalization of the thick disk. We look forward to the results of the next decade.

ACKNOWLEDGMENTS

The *Annual Review of Astronomy and Astrophysics* is online at
http://astro.annualreviews.org

LITERATURE CITED

Aannestad PA, Kenyon SJ, Hammond GL, Sion EM. 1993. *Astron. J.* 105:1033–44

Adams FC, Laughlin G. 1996. *Ap. J.* 468:586–97

Afonso C, Alard C, Albert JN, Andersen J, Ansari R, et al. 1998. *Astron. Astrophys.* 337: L17–20

Alberts C, Savonije GJ, van den Heuvel EPJ, Pols OR. 1996. *Nature* 380:676–676

Alcock C, Akerloff CW, Allsman RA, Axelrod TS, Bennett DP, et al. 1993. *Nature* 365:621–23

Alcock C, Allsman RA, Alves D, Axelrod TS, Becker AC, et al. 1997. *Ap. J.* 486:697–726

Alcock C, Allsman RA, Alves D, Axelrod TS, Becker AC, et al. 2000. *Ap. J.* 541:281–307

Alcock C, Fristrom CC, Siegelman R. 1986. *Ap. J.* 302:462–76

Althaus LG, Serenelli AM, Benvenuto OG. 2001a. *Ap. J.* 554:1110–17

Althaus LG, Serenelli AM, Benvenuto OG. 2001b. *MNRAS* 323:471–83

Andreuzzi G, Richer HB, Limongi M, Bolte M. 2002. *Astron. Astrophys.* 390:961–65

Aubourg E, Bareyre P, Brehin S, Gros M, Lachiezo-Rey M, et al. 1993. *Nature* 365: 623–25

Bailyn CD. 1993. *Ap. J.* 411:L83–86

Barrat JL, Hansen CJ, Mochkovitch R. 1988. *Astron. Astrophys.* 199:L15–18

Beauchamp A. 1996. PhD thesis Université de Montréal

Bell JF, Bailes M, Bessell MS. 1993. *Nature* 364:603–5

Benvenuto OG, Althaus LG. 1999. *MNRAS* 303:30–38

Bergeron P. 2001. *Ap. J.* 558:369–76

Bergeron P. 2003. *Ap. J.* 586:201–9

Bergeron P, Leggett SK. 2002. *Ap. J.* 580:1070–76

Bergeron P, Leggett SK, Ruiz M-T. 2001. *Ap. J. Suppl.* 133:413–49

Bergeron P, Liebert J, Fulbright MS. 1995. *Ap. J.* 444:810–17

Bergeron P, Ruiz M-T, Leggett SK. 1997. *Ap. J. Suppl.* 108:339–87

Bergeron P, Saffer RA, Liebert J. 1992. *Ap. J.* 394:228–47

Bergeron P, Saumon D, Wesemael F. 1995. *Ap. J.* 443:764–79

Bergeron P, Wesemael F, Beauchamp A. 1995. *Publ. Astron. Soc. Pac.* 107:1047–54

Bergeron P, Wesemael F, Fontaine G. 1992. *Ap. J.* 387:288–93

Bergeron P, Wesemael F, Fontaine G, Liebert J. 1990. *Ap. J.* 351:L21–24

Bildsten L, Hall DM. 2001. *Ap. J.* 549:L219–22

Binney J, Merrifield M. 1998. *Galactic Astronomy.* Princeton, NJ: Princeton Univ. Press

Böhm K-H, Carson TR, Fontaine G, van Horn HM. 1977. *Ap. J.* 217:521–29

Bondi H, Hoyle F. 1944. *MNRAS* 104:273–82

Borysow A, Jorgensen UG, Zheng C. 1997. *Astron. Astrophys.* 324:185–95

Bradley PA. 2001. *Ap. J.* 552:326–39

Branch D, Livio M, Yungelson LR, Boffi FR, Baron E. 1995. *Publ. Astron. Soc. Pac.* 107:1019–29

Canal R, Isern J, Ruiz-Lapuente P. 1997. *Ap. J.* 488:L35–38

Castellani V, Luridiana V, Romaniello M. 1994. *Ap. J.* 428:633–37

Chabrier G. 1993. *Astroph. J.* 414:695–700

Chabrier G, Brassard P, Fontaine G, Saumon D. 2000. *Ap. J.* 543:216–26

Chabrier G, Ashcroft NW, De Witt B. 1992. *Nature* 360:48–50

Charlot S, Silk J. 1995. *Ap. J.* 445:124–32

Claver CF. 1995. PhD thesis. Univ. Texas, Austin

Claver CF, Liebert J, Bergeron P, Koester D. 2001. *Ap. J.* 563:987–98

Cool AM, Grindlay JE, Cohn HN, Lugger PM, Bailyn CD. 1998. *Ap. J.* 508:L75–78

Cool AM, Piotto G, King I. 1996. *Ap. J.* 468:655–62

Dahn CC, Liebert J, Harris HC, Guetter HH. 1995. In *The Bottom of the Main Sequence—and Beyond*, ed. CG Tinney, pp. 239–48. Berlin: Springer

D'Amico N, Possenti A, Fici L, Manchester RN, Lyne AG, et al. 2002. *Ap. J.* 570:L89–92

D'Antona F, Mazzitelli I. 1989. *Ap. J.* 347:934–49

D'Antona F, Mazzitelli I. 1990. *Annu. Rev. Astron. Astrophys.* 28:139–81

Danziger IJ, Baade D, Della Valle M. 1993. *Astron. Astrophys.* 275:382–88

Davies MB, Hansen BMS. 1998. *MNRAS* 301:15–24

Davies MB, King A, Ritter H. 2002. *MNRAS* 333:463–68

Dawson PC. 1986. *Ap. J.* 311:984–1000

de Jong J, Kuijken K, Neeser M. 2000. /astro-ph/0009058

Driebe T, Schönberner D, Blöcker T, Herwig F. 1998. *Astron. Astrophys.* 339:123–33

Drukier G. 1996. *MNRAS* 280:498–514

Dull JD, Cohn HN, Lugger PM, Murphy BW, Seitzer PO, et al. 1997. *Ap. J.* 481:267–81

Dupuis J, Fontaine G, Wesemael F. 1993. *Ap. J. Suppl.* 87:345–65

Edmonds PD, Grindlay JE, Cool A, Cohn HN, Lugger PM, et al. 1999. *Ap. J.* 516:250–62

Elson RAW, Gilmore GF, Santiago BX, Casertano S. 1995. *Astron. J.* 110:682–92

Elson RAW, Santiago BX, Gilmore GF. 1996. *New Ast.* 1:1–16

Faber SC, Gallagher JS. 1979. *Annu. Rev. Astron. Astrophys* 17:135–87

Fabrika S, Volyavin G. 1999. *11th Eur. Wkshp. White Dwarfs* ed. JE Solheim, EG Meistas, ASP Conf. Ser. 169, pp. 214–20. San Francisco: Astron. Soc. Pac.

Fan X. 1999. *Astron. J.* 117:2528–51

Festin L. 1998. *Astron. Astrophys.* 336:883–94

Fields BD, Mathews GJ, Schramm DN. 1997. *Ap. J.* 483:625–37

Finley DS, Koester D, Basri G. 1997. *Ap. J.* 488:375–96

Flynn C, Gould A, Bahcall JN. 1996. *Ap. J.* 466:L55–58

Flynn C, Holopainen J, Holmberg J. 2002. /astro-ph/0202244

Flynn C, Sommer-Larsen J, Fuchs B, Graff DS, Salim S. 2001. *MNRAS* 322:553–60

Flynn C, Holopainen J, Holmberg J. 2003. *MNRAS* 339:817–24

Fontaine G, Brassard P. 2002. *Ap. J.* 581:L33–36

Fontaine G, Brassard P, Bergeron P. 2001. *Publ. Astron. Soc. Pac.* 113:409–35

Fontaine G, Thomas JH, Van Horn HM. 1973. *Ap. J.* 184:911–16

Fontaine G, Van Horn HM. 1976. *Ap. J. Suppl.* 31:467–87

Garcia-Berro E, Hernanz M, Isern J, Mochkovitch R. 1988. *Nature* 333:642–44

Garcia-Berro E, Hernanz M, Isern J, Chabrier G, Segretain L, et al. 1996. *Astron. Astrophys. Suppl.* 117:13–18

Gerssen J, van der Marel RP, Gebhardt K, Guhathakurta P, Peterson RC, et al. 2003. *Astron. J.* 124:3270–88; 124:376–77

Gibson BK, Mould J. 1997. *Ap. J.* 482:98–103

Goldman B, Afonso C, Alard C, Albert J-N, Amadon A, et al. 2002. *Astron. Astrophys.* 389:L69–73

Gould A, Flynn C, Bahcall JN. 1998. *Ap. J.* 503:798–808

Graff DS, Freese K, Walker TP, Pinsonneault MH. 1999. *Ap. J. Lett.* 523:L77–80

Graff DS, Laughlin G, Freese K. 1998. *Ap. J.* 499:7–19

Greenstein JL. 1986. *Ap. J.* 304:334–55

Greenstein JL, Liebert JW. 1990. *Ap. J.* 360:662–84

Gyuk G, Gates E. 1999. *MNRAS* 304:281–87

Hambly NC, et al. 2001a. *MNRAS* 326:1279–94

Hambly NC, Irwin MJ, MacGillivray HT. 2001b. *MNRAS* 326:1295–314

Hambly NC, Davenhall AC, Irwin MJ, MacGillivray HT. 2001c. *MNRAS* 326:1315–27

Hambly NC, Smartt SJ, Hodgkin ST. 1997. *Ap. J.* 489:L157–60

Han Z, Podsiadlowski P, Eggleton PJ. 1994. *MNRAS* 270:121–30

Hansen BMS. 1998. *Nature* 394:860–62

Hansen BMS. 1999a. *Ap. J.* 520:680–95

Hansen BMS. 1999b. *Ap. J.* 517:L39–42

Hansen BMS. 2001. *Ap. J.* 558:L39–42

Hansen BMS, Brewer J, Fahlman GG, Gibson BK, Ibata R, et al. 2002. *Ap. J.* 574:L155–58

Hansen BMS. 2003. *Ap. J.* 582:915–18

Hansen BMS, Kalogera V, Rasio FA. 2003. *Ap. J.* 586:1364–73

Hansen BMS, Phinney ES. 1998. *MNRAS* 294:569–81

Harris HC, Dahn CC, Vrba FJ, Henden AA, Liebert J, et al. 1999. *Ap. J.* 524:1000–7

Harris HC, Hansen BMS, Liebert J, Vanden-Berk DE, Anderson SF, et al. 2001. *Ap. J.* 549:L109–12

Hegyi DJ, Olive KA. 1986. *Ap. J.* 303:56–65

Hernanz M, Garcia-Berro E, Isern K, Mochkovitch R, Segretain L, et al. 1994. *Astroph. J.* 434:652–61

Hodgkin ST, Oppenheimer BR, Hambly NC, Jameson RF, Smartt SJ, Steele IA. 2000. *Nature* 403:57–59

Holberg JB, Oswalt T, Sion EM. 2002. *Ap. J.* 571:512–18

Hummer DG, Mihalas D. 1988. *Ap. J.* 331:794–814

Ibata RA, Irwin M, Bienayme O, Scholz R, Guibert J. 2000. *Ap. J.* 532:L41–44

Ibata RA, Richer HB, Gilliland RL, Scott D. 1999. *Ap. J.* 524:L95–98

Iben I, Laughlin G. 1989. *Ap. J.* 341:312–26

Iben I, Tutukov AV. 1984a. *Ap. J. Suppl.* 54:335–72

Iben I, Tutukov AV. 1984b. *Ap. J.* 282:615–30

Iben I, Tutukov AV. 1986. *Ap. J.* 311:742–52

Ichimaru S, Iyetomi H, Ogata S. 1988. *Ap. J.* 334:L17–20

Iglesias CA, Rogers FJ, Saumon D. 2002. *Ap. J.* 569:L111–14

Illarionov AF, Sunyaev RA. 1975. *Astron. Astrophys.* 39:185–95

Isern J, Hernanz M, Mochkovitch R, Garcia-Berro E. 1991. *Astron. Astrophys.* 241:L29–32

Isern J, Garcia-Berro E, Hernanz M, Chabrier G. 2000. *Ap. J.* 528:397–400

Jorgensen UG, Borysow A, Höfner S, Wing RF. 2000. *Astron. Astrophys.* 361:283–92

Kalirai JS, Ventura P, Richer HB, Fahlman GG, Durrell PR, et al. 2001. *Astron. J.* 122:3239–57

Kawka A, Vennes S, Wickramasinghe DT, Schmidt GD, Koch R. 2003. In *Proc. 13th Eur. Wkshp. White Dwarfs*, ed. R. Silvotti D. de Martino, Dordrecht, Neth: Kluwer Academic. In press

Kepler SO, Mukadam A, Winget DE, Nather

RE, Metcalfe TS, et al. 2000. *Ap. J.* 534: L185–88

Koester D. 2002. *Astron. & Astrophys. Rev.* 11: 33–67

Koester D, Schulz H, Weidemann V. 1979. *Astron. Astrophys.* 76:262–75

King I, Anderson J, Cool AM, Piotto G. 1998. *Ap. J.* 492:L37–40

Kippenhahn R, Kohl K, Weigert A. 1967. *Z. Ap.* 66:58–79

Knox RA, Hawkins MRS, Hambly NC. 1999. *MNRAS* 306:736–52

Koester D, Chanmugam G, Reimers D. 1992. *Ap. J.* 395:L107–10

Koester D, Schönberner D. 1986. *Astron. Astrophys.* 154:125–34

Koester D, Schulz H, Weidemann V. 1980. *Astron. Astrophys.* 6:262–75

Koopmans LVE, Blandford RD. 2001. /astro-ph/0107358

Kulkarni SR. 1986. *Ap. J.* 306:L85–88

Lamb DQ, Van Horn HM. 1975. *Ap. J.* 200: 306–23

Larson RA. 1987. *Com. Ap.* 11:273–82

Leggett SK, Ruiz M-T, Bergeron P. 1998. *Ap. J.* 497:294–302

Lépine S, Shara MM, Rich RM. 2002. *Astron. J.* 124:1190–212

Liebert J. 1988. *Publ. Astron. Soc. Pac.* 100:1302–5

Liebert J, Bergeron P, Holberg JB. 2003. *Astron. J.* 125:348–53

Liebert J, Dahn CC, Gresham M, Stritmatter PA. 1979. *Ap. J.* 233:226–38

Liebert J, Dahn CC, Monet DG. 1988. *Ap. J.* 332:891–909

Liebert J, Dahn CC, Monet DG. 1989. In *White Dwarfs*, Proc. IAU Colloq. 114, ed. G Wegner, p. 15. Berlin: Springer

Liebert J, Sion EM. 1979. *Astrophys. Lett.* 20:53–55

Liebert J, Wesemael F, Hansen CJ, Fontaine G, Shipman HL, et al. 1986. *Ap. J.* 309:241–52

Lorimer DR, Lyne AG, Festin L, Nicastro L. 1995. *Nature* 376:393

Lundgren SC, Cordes JM, Foster RS, Wolszszan A, Camilo F. 1996. *Ap. J.* 458:L33–36

Luyten WJ. 1922. *Publ. Astron. Soc. Pac.* 34:156–60

Luyten WJ. 1975. *LHS catalogue*. Minneapolis, MN: Univ. Minn.

Luyten WJ. 1979–1980. *New Luyten Catalogue of Stars with Proper Motions Larger than Two tenths of an Arcsecond*, Vols. 1–4. Minneapolis, MN: Univ. Minn.

Lynden-Bell D, Tout CA. 2001. *Ap. J.* 558: 1–9

Maddox SJ, Sutherland WJ, Efstathiou G, Loveday J. 1990. *MNRAS* 243:692–712

Majewski SR, Siegel MH. 2002. *Ap. J.* 569: 432–45

Malo A, Wesemael F, Bergeron P. 1999. *Ap. J.* 517:901–5

Marsh MC, Barstow MA, Buckley DA, Burleigh MR, Holberg JB, et al. 1997. *MNRAS* 287:705–21

Marsh TR, Dhillon VS, Duck SR. 1995. *MNRAS* 275:828–40

Maxted PFL, Marsh TR. 1998. *MNRAS* 296: L34–37

May A, Binney J. 1986. *MNRAS* 221:857–77

Méndez RA, Minniti D. 2000. *Ap. J.* 529:911–16

Méndez RA, Minniti D, de Marchi G, Baker A, Couch WJ. *MNRAS* 283:666–72

Metcalfe TR, Salaris M, Winget DE. 2002. *Ap. J.* 573, 803–11

Metcalfe TR, Winget DE, Charbonneau P. 2001. *Ap. J.* 557:1021–27

Mochkovitch R. 1983. *Astron. Astrophys.* 122:212–18

Monet DG, Fisher MD, Liebert J, Canzian B, Harris HC, et al. 2000. *Astron. J.* 120:1541–47

Montgomery MH, Klumpe EW, Winget DE, Wood MA. 1999. *Astrophys. J.* 525:482–91

Montgomery MH, Winget DE. 1999. *Ap. J.* 526:976–90

Mould J, Liebert J. 1978. *Ap. J.* 226:L29–32

Nelson CA, Cook KH, Axelrod TS, Mould JR, Alcock C. 2002. *Ap. J.* 573:644–661

Oppenheimer BR, Hambly NC, Digby AP, Hodgkin ST, Saumon D. 2001a. *Science* 292:698–702

Oppenheimer BR, Saumon D, Hodgkin ST,

Jameson RF, Hambly NC. 2001b. *Ap. J.* 550:448–56

Ostriker JP, Peebles PJE. 1973. *Ap. J.* 186:467–80

Oswalt TD, Smith JA, Wood MA, Hintzen P. 1996. *Nature* 382:692–94

Paresce F, de Marchi G, Romaniello M. 1995. *Ap. J.* 440:216–26

Pelletier C, Fontaine G, Wesemael F, Michaud G, Wegner G. 1986. *Ap. J.* 307:242–52

Phinney ES. 1993. In *Structure & Dynamics of Globular Clusters*, ed. SG Djorgovski, G Meylan, 50:141–69. San Francisco: Astron. Soc. Pac.

Provencal JL, Shipman HL, Hog E, Thejll P. 1998. *Ap. J.* 494:759–67

Provencal JL, Shipman HL, Koester D, Wesemael F, Bergeron P. 2002. *Ap. J.* 568:324–34

Provencal JL, Shipman HL, Wesemael F, Bergeron P, Bond HE, et al. 1997. *Ap. J.* 480:777–83

Reid IN. 1996. *Astron. J.* 111:2000–16

Reid IN, Majewski SR. 1993. *Ap. J.* 409:635–62

Reid IN, Sahu KC, Hawley SL. 2001. *Ap. J.* 559:942–47

Renzini A, Bragaglia A, Ferraro FR, Gilmozzi R, Ortolani S, et al. 1996. *Ap. J.* 465:L23–26

Reylé C, Robin AC, Crézé M. 2001. *Astron. Astrophys.* 378:L53–56

Richer HB. 2003. In *Proc. The Dark Universe: Matter, Energy & Gravity*, ed. M. Livio. Cambridge, UK: Cambridge Univ. Press. In press. /astro-ph/0107079

Richer HB, Fahlman GG, Ibata R, Stetson PB, Bell RA, et al. 1995. *Ap. J.* 451:L17–20

Richer HB, Fahlman GG, Ibata R, Pryor C, Bell RA, et al. 1997. *Ap. J.* 484:741–60

Richer HB, Brewer J, Fahlman GG, Gibson BK, Hansen BMS, et al. 2002. *Ap. J.* 574:L151–54

Richer HB, Fahlman GG. 1988. *Ap. J.* 325:218–24

Richer HB, Fahlman GG, Rosvick J, Ibata R. 1998. *Ap. J.* 504:L91–94

Rubin VC, Ford WK Jr, Thonnard N. 1978. *Ap. J. Lett.* 225:L107–10

Ruiz M-T, Takamiya MY. 1995. *Astron. J.* 109:2817–20

Ryu D, Olive KA, Silk J. 1990. *Ap. J.* 353:81–89

Sahu KC. 1994. *Nature* 370:275

Salaris M, Dominguez I, Garcia-Berro E, Hernanz M, Isern J, Mochkovitch R. 1997. *Ap. J.* 486:413–19

Salaris M, Garcia-Berro E, Hernanz M, Isern J, Saumon D. 2000. *Ap. J.* 544:1036–43

Salim S, Gould A. 2002. *Ap. J.* 575:L83–86

Salpeter EE. 1992. *Ap. J.* 393:258–65

Saumon D, Jacobsen SB. 1999. *Ap. J.* 511: L107–10

Schmidt M. 1959. *Ap. J.* 129:243–58

Schmidt GD, Bergeron P, Fegley Jr B. 1995. *Ap. J.* 43:274–80

Schönberner D, Driebe T, Blöcker T. 2000. *Astron. Astrophys.* 356:929–34

Segretain L. 1996. *Astron. Astrophys.* 310:485–88

Segretain L, Chabrier G. 1993. *Astron. Astrophys.* 271:L13–16

Segretain L, Chabrier G, Hernanz M, Garcia-Berro E, Isern J, Mochkovitch R. 1994. *Ap. J.* 434:641–51

Shaviv G, Kovetz A. 1976. *Astron. Astrophys.* 51:383–91

Shipman HL, Liebert J, Green RF. 1987. *Ap. J.* 315:239–50

Shipman HL, Provencal JL, Hog E, Thejll P. 1998. *Ap. J.* 488:L43–46

Shipman HL, Sass CA. 1980. *Ap. J.* 235:177–85

Silk J. 1991. *Science* 251:537–41

Silvestri NM, Oswalt TD, Hawley SL. 2002. *Astron. J.* 124:1118–26

Silvestri NM, Oswalt TD, Wood MA, Smith JA, Reid IN, Sion EM. 2001. *Astron. J.* 121:503–16

Sion EM. 1984. *Ap. J.* 282:612–14

Smith JA, Oswalt TD. 1994. In *The Bottom of the Main Sequence—and Beyond*, ed. CG Tinney, pp. 113–19. Heidelberg: Springer-Verlag

Stevenson DJ. 1980. *J. Phys. Soc.* 41:C61–64

Straniero O, Dominguez I, Imbriani G, Piersanti L. 2003. *Ap. J.* 583:878–84

Stringfellow G, De Witt HE, Slattery WL. 1990. *Phys. Rev. A* 41:1105–11

Tamanaha CM, Silk J, Wood MA, Winget DC. 1990. *Ap. J.* 358:164–69

Taylor JM, Grindlay JE, Edmonds PD, Cool AM. 2001. *Ap. J.* 553:L169–72

Tokunaga A, Becklin EE, Zuckerman B. 1990. *Ap. J.* 358:L21–24

van Kerkwijk MH, Bell JF, Kaspi VM, Kulkarni SR. 2000. *Ap. J.* 530:L37–40

van Kerkwijk MH, Bergeron P, Kulkarni SR. 1996. *Ap. J.* 467:L89–92

Vennes S. 1999. *Ap. J.* 525:995–1007

Vennes S, Thejll PA, Genova Galvan R, Dupuis J. 1997. *Ap. J.* 480:714–34

Von Hippel T. 1998. *Astron. J.* 115:1536–42

Von Hippel T, Gilmore G. 2000. *Astron. J.* 120:1384–95

Von Hippel T, Gilmore G, Jones DHP. 1995. *MNRAS* 273:L39–42

Webbink RF. 1975. *MNRAS* 171:555–68

Weidemann V. 1990. *Annu. Rev. Astron. Astrophys.* 28:103–37

Wesemael F, Truran J. 1982. *Ap. J.* 260:807–14

Williams RE, Blacker B, Dickinson M, Dixon WV, Ferguson HC, et al. 1996. *Astron. J.* 112:1335–89

Winget DE, Hansen CJ, Liebert J, Van Horn HM, Fontaine G, et al. 1987. *Ap. J.* 315:L77–80

Winget DE, Kepler SO, Kanaan A, Montgomery MH, Giovannini O. 1997. *Ap. J.* 487:L191–94

Wolff B, Koester D, Liebert J. 2002. *Astron. Astrophys.* 385:995–1007

Wood MA. 1992. *Ap. J.* 86:539–61

Wood MA. 1995. *Proc. 9th Eur. Wrkshp. White Dwarfs*, ed. D. Koester, K Werner, 43:41–45. Heidelberg: Springer-Verlag

Wood MA, Oswalt TD. 1998. *Ap. J.* 497:870–82

York DG, Adelman J, Anderson JE, Anderson SF, Annis J, et al. 2000. *Astron. J.* 120:1579–87

Yuan JW. 1989. *Astron. Astrophys.* 224:108–16

Zoccali M, Renzini A, Ortolani S, Bragaglia A, Bohlin R, et al. 2001. *Ap. J.* 553:733–43

Zuckerman B, Becklin EE. 1987. *Nature* 330:138–40

Zuckerman B, Becklin EE. 1992. *Ap. J.* 386:260–64

Zuckerman B, Koester D, Reid IN, Hüsch 2003. *Ap. J.* Submitted

Zuckerman B, Reid IN. 1998. *Ap. J.* 505:L143–146
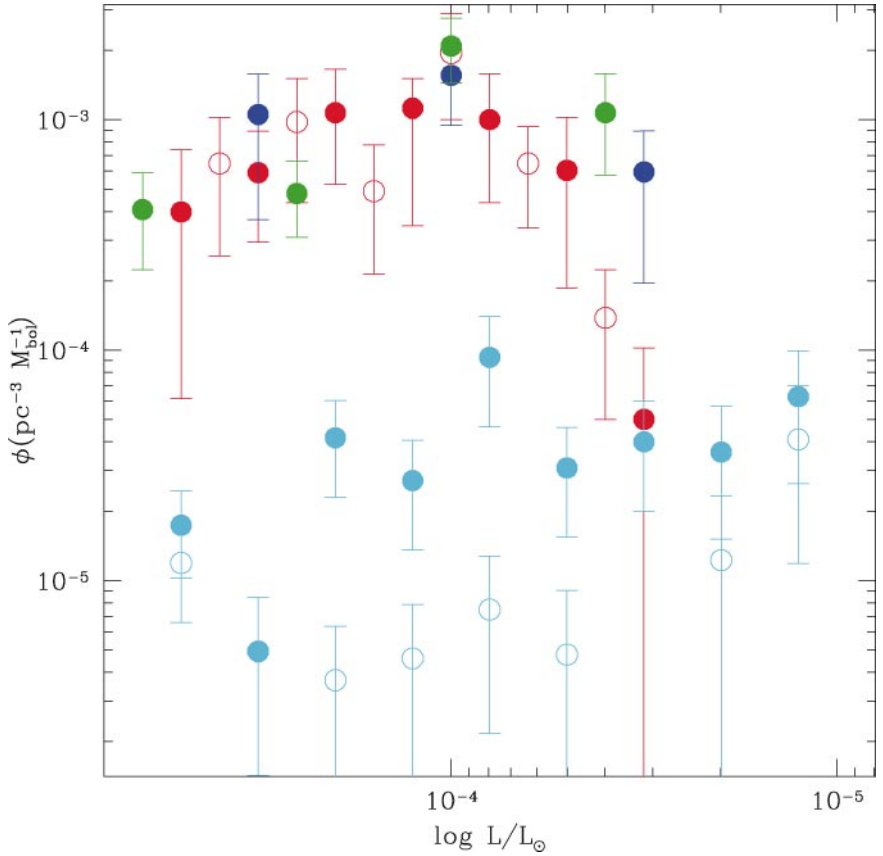
Figure 3 The red, blue and green points indicate the disk white dwarf luminosity functions of Leggett, Ruiz & Bergeron (1998), Oswalt et al. (1996) and Knox, Hambly & Hawkins (1999). (The Leggett et al. sample is represented twice, as solid and open symbols, with different binning). The cyan points solid below represent the luminosity function of high velocity white dwarfs ($V_\perp > 94$ km.s^{-1}) from Oppenheimer et al. (2001). The open points show the luminosity function for a velocity cut of $V_\perp > 141$ km.s^{-1}.
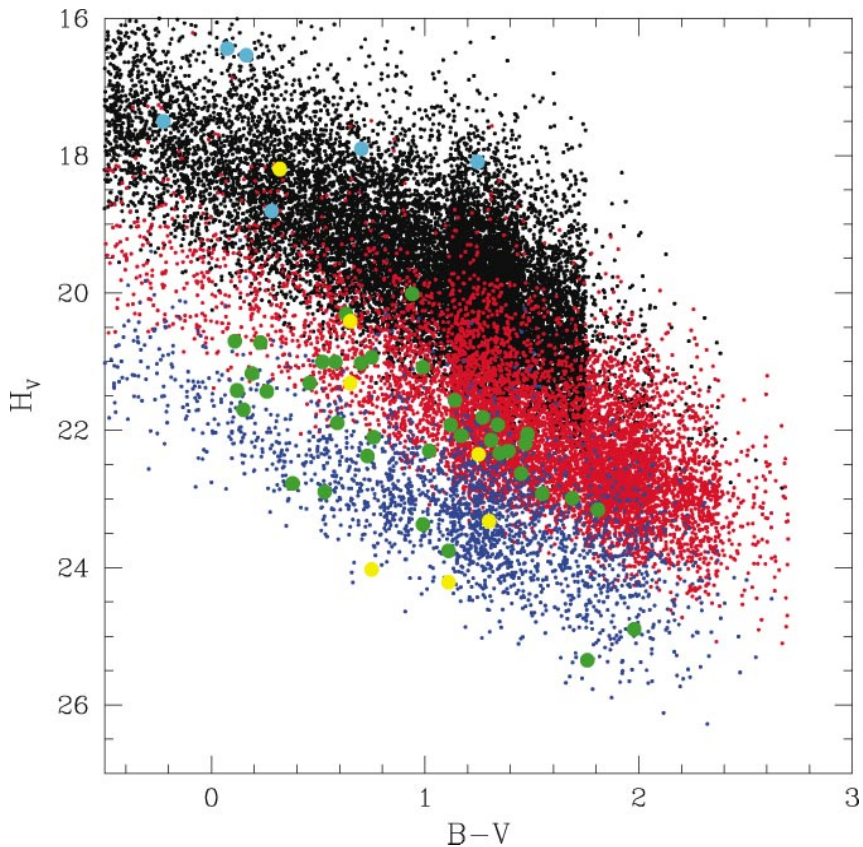
Figure 6 The small black points are thin disk stars, the red points are thick disk stars, and the blue are halo objects. The green points are from OHDHS, where we have used the B_J-$R59F$ color as a proxy for *B-V*. A significant fraction of the Oppenheimer sample fall in the intermediate region where both thick disk and halo stars can contribute. Some fraction of the OHDHS sample are likely halo stars. The cyan points are the data from Majewski & Siegel (2001) and are clearly thin disk stars. The large yellow points are from the Groth strip study of Nelson et al. (2000). These observations were made in the V-I color and have been transformed to V-I assuming pure hydrogen model atmospheres and standard transformations from HST to ground-based systems. This sample thus also represents a mix of thick disk and halo stars.
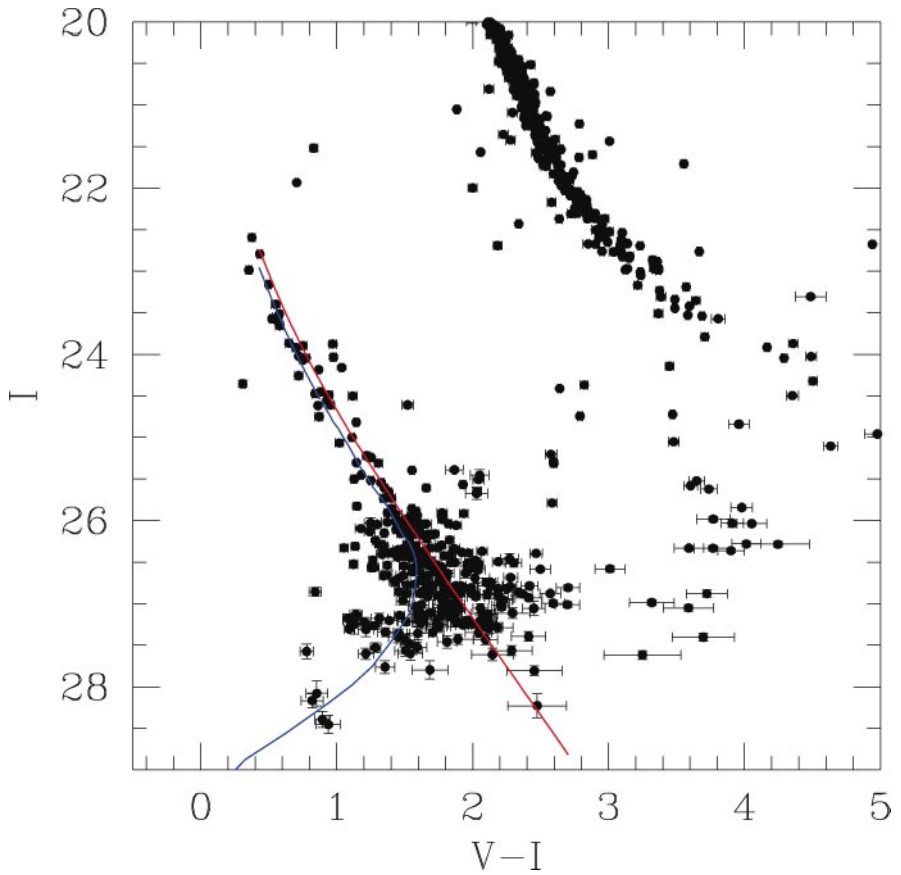
Figure 8 Cluster members are shown, with approximate photometric error bars. The red and blue curves are cooling sequences for a 0.6 $M_\odot$ white dwarf with pure helium and pure hydrogen atmospheres, respectively.

Contents

ERRATA

An online log of corrections to *Annual Review of Astronomy and Astrophysics* chapters (if any, 1997 to the present) may be found at http://astro.annualreviews.org/errata.shtml